NRL Report 6532

A Note on the Polarization and Phase Characteristics of Radio Waves Propagating Through the Lower Ionosphere

JOHN M. GOODMAN

Search Radar Branch
Radar Division

June 5, 1967

NAVAL RESEARCH LABORATORY
Washington, D.C.

DISTRIBUTION OF THIS DOCUMENT IS UNLIMITED

CONTENTS

Abstract	ii
Problem Status	ii
Authorization	ii
INTRODUCTION	1
FARADAY ROTATION	1
Case 1 - Moving Reference Point	3
Case 2 - Fixed Reference Point	19
PHASE SCINTILLATION	28
CONCLUSION	32
ACKNOWLEDGMENTS	33
REFERENCES	33

ABSTRACT

Some ionospheric radio propagation problems associated with the satellite radar situation have been examined for radar frequencies between 100 and 1000 Mc/s. It has been shown that the maximum number of fades exhibited by a train of radar pulses is governed by the quantity $\overline{H \csc I}$, where H is the magnetic field intensity and I is the magnetic field inclination, except near the magnetic equator. At 100 Mc/s the maximum number of fades is characteristically less than 50, and since the Faraday rotation is inversely proportional to the square of the radar frequency, only one-half of a fade should be observed at 1000 Mc/s.

Faraday rotational signal degradation of a linearly polarized radar signal has been shown to be negligible at 1000 Mc/s except possibly during winter days at sunspot maximum. In all but possibly the polar region, it is suggested that the relationship between irregularity scale ΔL and phase excursion $\Delta\delta$ is given by

$$\frac{\Delta L}{\Delta\delta \cdot n_f} \approx 10^3,$$

where ΔL is in meters, $\Delta\delta$ is in radians, and n_f is the radar frequency in hundreds of megacycles per second.

PROBLEM STATUS

This is a final report on the problem; work on the problem is completed. Unless otherwise notified the problem will be closed 30 days after the issuance of this report.

AUTHORIZATION

NRL Problem R07-16
Project RT 7042-045/6521/F019-02-18

Manuscript submitted December 22, 1966.

A NOTE ON THE POLARIZATION AND PHASE CHARACTERISTICS OF RADIO WAVES PROPAGATING THROUGH THE LOWER IONOSPHERE

INTRODUCTION

It is well established that the earth's ionosphere—extending between roughly 100 and 1000 kilometers above sea level—is a magneto-ionic medium and, as such, perturbs the polarization and phase characteristics of satellite radio waves transmitted toward the earth. The rotation of the plane of polarization of a linearly polarized radio wave is proportional to the product of the readily determined magnetic field parameter (M-factor)* and the electron content along the radio path and is inversely proportional to the square of the radio frequency. The time rate of change of this rotational effect—often called the Faraday effect by virtue of its optical analog—defines the signal fading rate and has been used successfully to deduce the electron content of the ionosphere.

Since the refractive index of the ionosphere at vhf and above lies between zero and unity, it follows that radio waves in that frequency domain have a phase velocity which is in excess of the free-space speed of light. Similarly, the length of phase path traversed by the radio wave is reduced with respect to free space. This phenomenon is closely related to the scintillation of phase, angle of arrival, range, and signal amplitude in the presence of ionospheric inhomogeneities. These effects have been studied by Lawrence et al. (1) and Millman (2).

Other perturbations for the radar case include group path delay of a radar signal and ionospherically induced pulse distortion. Differential effects and absorption are predominantly measurable only in the hf domain and are not considered in this report.

This report is primarily concerned with the estimation of Faraday rotation and phase distortion of radar pulses in the 100 Mc/s to 1000 Mc/s frequency domain. In the Faraday analysis particular emphasis is placed upon polar orbiting satellite radars, since they exhibit the greatest worldwide coverage. The Faraday rotation predictions are based upon variable beam orientations, assuming a satellite altitude of 300 kilometers, and the worldwide maximum Faraday rotation is estimated for the frequency range under consideration and presented on global charts. Although the precise satellite altitude is not critical in the process of estimating the gross Faraday effect, it is an important factor in the estimation of fine-scale phase effects. Phase effects as a function of frequency are estimated by extrapolating available fine-scale ionospheric data.

FARADAY ROTATION

Two distinct situations are encountered upon consideration of the average Faraday rotation problem, and they are illustrated in Figs. 1 and 2. Figure 1 depicts the satellite radar case for which there is no variation of the beam nadir angle (complement of the beam depression angle) and the surface reference point describes a great circle path which is approximately coincident with the subsatellite path. Azimuthal variations (referenced to geographic north) are defined by a fixed beam inclination with respect to the satellite velocity vector as measured in the horizontal plane. Figure 2 depicts the standard geometry associated with the amount of Faraday fading which occurs over a particular field station. For a detailed discussion of this geometry, the reader should

*The M-factor was first defined by Yeh and Gonzales (3) and has been discussed by a number of investigators including the author (4).

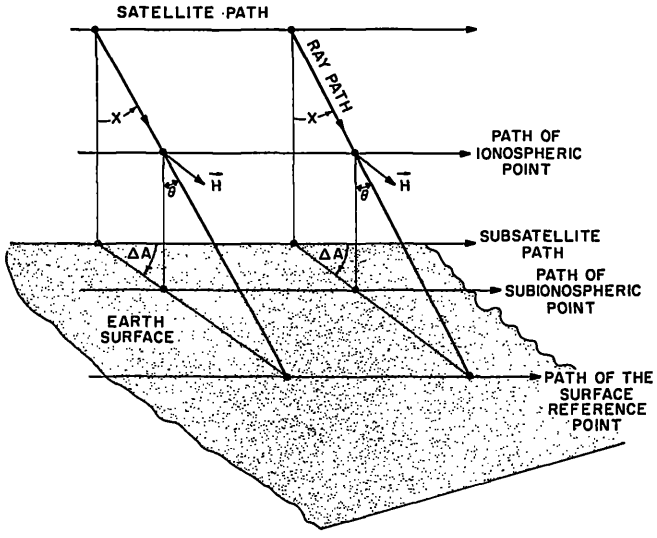

Fig. 1 - Geometry associated with a fixed ray path orientation with respect to the satellite velocity vector. It is assumed that the radio wave is earth-directed such that $X \leq 90°$.

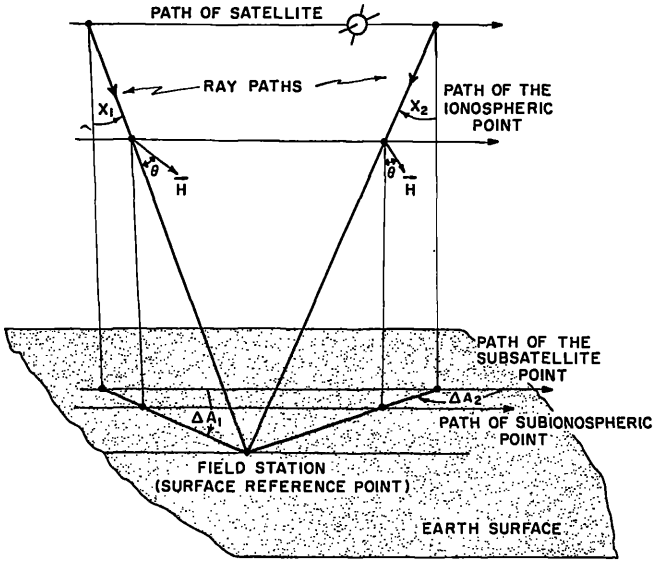

Fig. 2 - Geometry associated with a time-varying ray path orientation. This might correspond to a situation in which a stationary surface point (field station) is being "tracked" by a satellite radar.

refer to NRL Report 6234 (4). The general situation for which the beam azimuth and nadir are arbitrary may be represented by a composite of Figs. 1 and 2. A possible satellite radar situation in which a target is acquired and subsequently tracked is an example of the union of the two geometrical cases which are considered to be sufficiently dissimilar to warrant treatment separately.

Case 1 - Moving Reference Point

For the purpose of deducing the time variation of the magnetic field parameter ($\bar{\psi} = \overline{H \cos\theta \sec\chi}$) for a hypothetical satellite, a modification in an existing Fortran magnetic field model program was made. The inputs to the program were geographic latitude and longitude, beam azimuth and nadir, and altitude $\bar{h}$ of the ionospheric point. The outputs of the program include the propagation angle (the angle between the ray path and the magnetic field vector) θ, the magnetic inclination I, and the magnetic declination D, as well as $\bar{\psi}$.

The symbol ΔA represents the beam azimuth with respect to the satellite velocity vector and is measured in the clockwise sense. The true azimuth of the center of the radar beam A is given by the sum of ΔA and the velocity vector azimuth—denoted by the symbol A_v—and is also measured in the clockwise sense. Figure 3 is a plot of $A_v(t)$ for a polar satellite in circular orbit having a period of 95 minutes and an inclination of 81.5 degrees. The subsatellite latitude function $\lambda(t)$ corresponding to $A_v(t)$ and ΔA is depicted in Fig. 4 along with the relative longitude function $\Delta\phi(t)$.

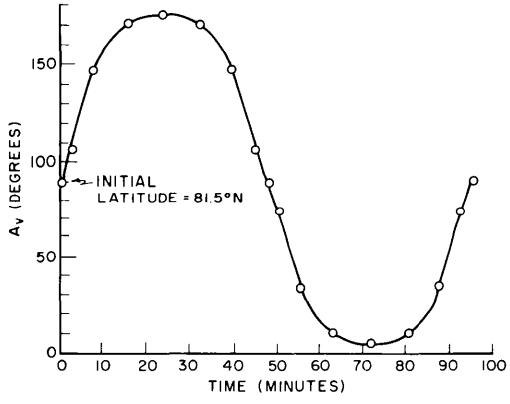

Fig. 3 - The velocity vector azimuth A_V as a function of satellite (rather than subsatellite) time. It is assumed that the orbital period is 95 minutes, the inclination is 81.5°, and the orbit is circular.

Computations of $\bar{\psi}$ were made for a complete orbit of the satellite, assuming some initial longitude ϕ_0 and an initial latitude λ_0 = 81.5°, for values of $\bar{h}$ = 100, 200, 300, 400, and 500 kilometers, for values of beam nadir χ = 0°, 15°, 30°, 45°, 60°, and 75°, and values of beam azimuth ΔA = -45°, 0°, and 45°. In addition, ϕ_0 was varied in steps of 10° from the Greenwich meridian such that ϕ_0 = 0°E, 10°E, 20°E,... . Before analyzing these computations it will be instructive to discuss the selection of the so-called ionospheric point.

It is well known that the amount of Faraday rotation at very high frequencies is given by the equation

$$\Omega = 5.94 \times 10^{-2} f^{-2} \int_{h_1}^{h_2} H \cos\theta \sec\chi \, N \, dh, \tag{1}$$

where h_1 and h_2 are the altitudes of the radar and reflecting object respectively. The rotation in radians is in the clockwise sense as the radiowave progresses from the radar to the target provided a component of $\vec{H}$ exists which is directed toward the target. As the reflected radio wave returns to the radar, the plane of polarization rotates in the counterclockwise sense since the path of progression is now opposed to $\vec{H}$. The result is that twice as much clockwise rotation is observed over a two-way path as over a one-way path; i.e., the return trip does not negate the rotation incurred over the one-way path. If $\vec{H}$ is opposed to the transmitted radar beam direction, the total rotation is of course counterclockwise. Figure 5 depicts the variation of $\psi = H \cos\theta \sec\chi$ at the NRL Randle Cliff Radar site near Chesapeake Beach, Maryland (38°39'37"N, 76°32' 9"W) along a number of selected ray paths.

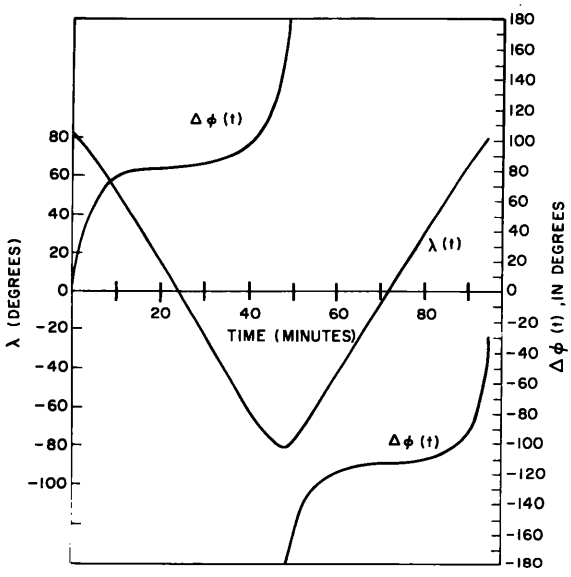

Fig. 4 - Subsatellite latitude λ and relative longitude Δφ as functions of satellite time

Since ψ is a continuous function of altitude and since N is everywhere positive, one may invoke the theorem of the mean to obtain a more convenient form of Eq. (1) in which the parameter ψ and the electron density N are embodied in two distinct and separate quantities. That is,

$$\Omega = 5.94 \times 10^{-2} f^{-2} \bar{\psi}(h_m) \int_{h_1}^{h_2} N \, dh, \tag{2}$$

where

$$\int_{h_1}^{h_2} N \, dh$$

is the electron content between the radar and the target, h_m is the altitude of the ionospheric point, and $\bar{\psi}(h_m)$ is given by

$$\bar{\psi}(h_m) = \frac{\int_{h_1}^{h_2} N(h)\, \psi(h)\, dh}{\int_{h_1}^{h_2} N(h)\, dh}. \tag{3}$$

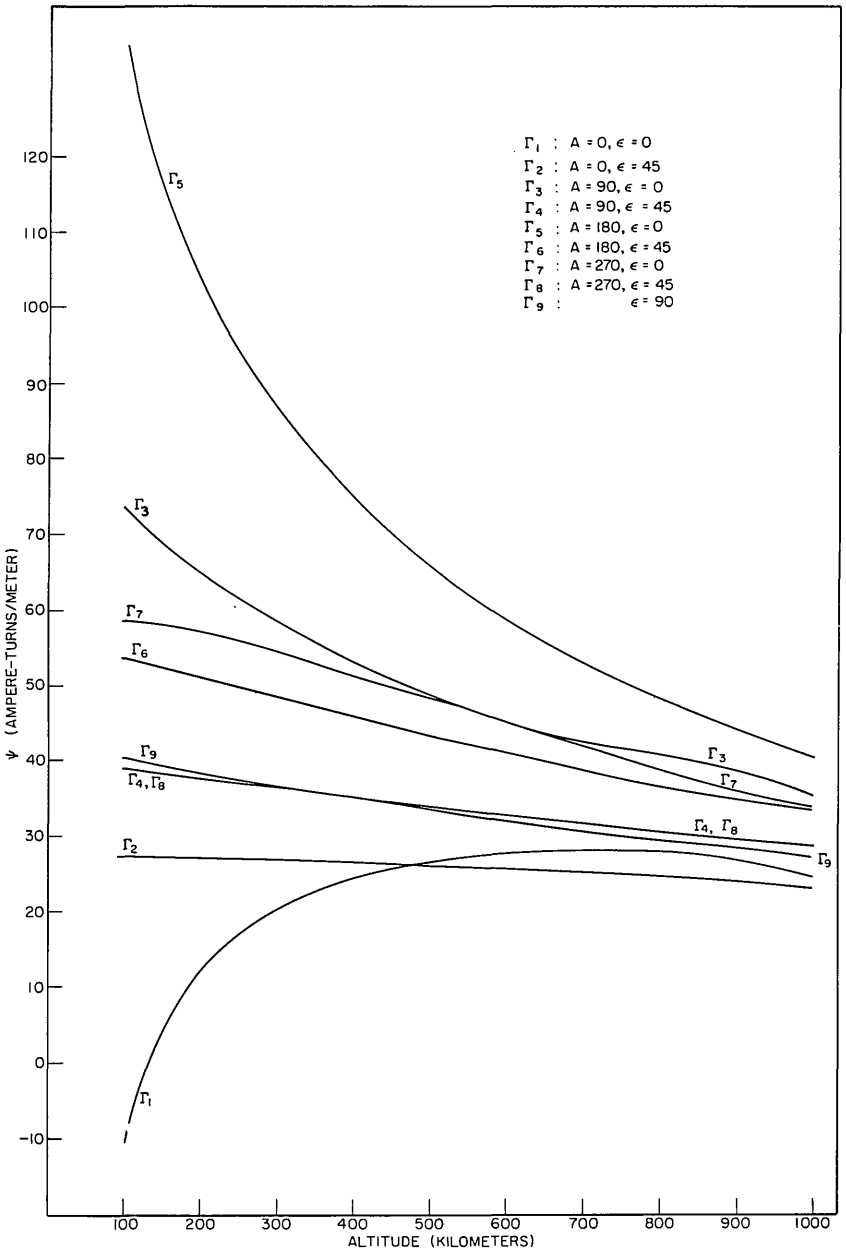

Fig. 5 - Variation of $H \cos\theta \sec\chi$ for a number of ray paths

If h_m, which defines the ionospheric point, is known a priori, it is clear that $\bar{\psi}$ need not be evaluated by means of Eq. (3). Assuming that $\psi(h)$ is linear between h_1 and h_2 such that

$$\psi(h) = \psi(h_1) + \frac{\partial\psi}{\partial h}(h - h_1),$$

it follows by substitution into Eq. (3) that

$$\bar{\psi}(h_m) = \psi(h_1) + \frac{\partial\psi}{\partial h}\left[\frac{\int_{h_1}^{h_2} hN(h)\,dh}{\int_{h_1}^{h_2} N(h)\,dh} - h_1\right] \tag{4}$$

but

$$\frac{\int_{h_1}^{h_2} hN\,dh}{\int_{h_1}^{h_2} N\,dh}$$

is simply the ionospheric mean $\bar{h}$. Consequently, if $\psi(h)$ is linear $h_m \equiv \bar{h}$ and $\bar{\psi}$ is simply defined apart from the magnetic field characteristics such as $\partial\psi/\partial h$ and ψ.

The Chapman formulation for $N(h)$ (5) embodies a host of simplifying assumptions which are not fulfilled (6) but surprisingly enough does represent the average ionosphere reasonably well. The normalized Chapman distribution may be written as

$$Ch(\delta h, H_s) = N(\delta h, H_s)/NF2 = \exp\left[\frac{1 - \left(\frac{\delta h}{H_s}\right) - \exp\left(-\frac{\delta h}{H_s}\right)}{2}\right], \tag{5}$$

where $NF2$ is the peak electron density in the F layer, $N(\delta h, H_s)$ is the electron density at the distance $\delta h = h - h_{F2}$ from the $F2$ maximum, and H_s is the scale height of the distribution. Given the height of the $F2$ maximum, it is trivial to transform $N(\delta h, H_s)$ into $N(h, H_s)$. After the electron density distribution is defined, the ionospheric mean of that portion of the ionosphere which lies between the satellite and the target is also well defined. Figure 6 illustrates the Chapman profiles for values of H_s = 50, 60, 70, 80, 90, 100, 110, and 120 kilometers. According to Seddon (7) the scale height varies between 75 kilometers during nocturnal hours and 100 kilometers during the day in the northern midlatitudes

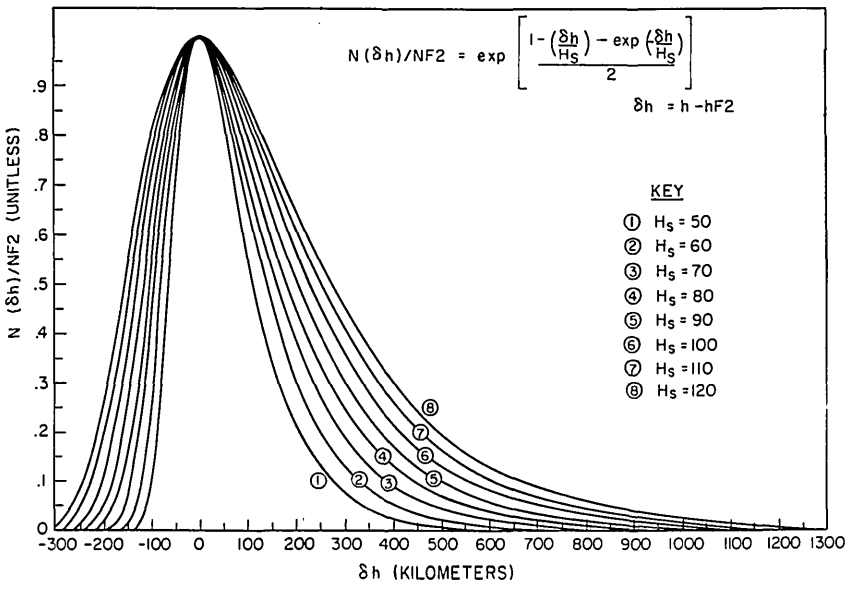

Fig. 6 - Chapman distributions of ionospheric electrons for values of H_s = 50, 60, 70, 80, 90, 100, 110, and 120 kilometers. The integral of the ordinate is known as the slab thickness, and the product of this integral with $NF2$ is called the electron content.

under undisturbed conditions. This matter is still open, however, since one would normally expect the upper-F-region scale height to increase with increasing darkness. If it is assumed that H_s = 100 kilometers and the satellite height is 300 kilometers—the nominal altitude of the $F2$ maximum—then $\bar{h} \approx$ 220 kilometers if the target is below the ionosphere. The value would naturally be higher if the target were embedded in the ionosphere. The exact placement of the ionospheric point is not too critical for Faraday rotation studies, since variations in $\bar{\psi}$ due to other effects such as ray path orientation changes are at least an order of magnitude larger.

It would be fallacious to compute $\bar{h}$ precisely, since the assumptions which are required throughout the calculations are not necessarily accurate. In fact, in most realistic analyses of satellite beacon data, one is fortunate to be able to specify $\bar{h}$ to within 25 kilometers with any confidence. For the purpose of this report we shall assume that the satellite altitude is 300 kilometers and that the ionospheric point is fixed at an altitude of 200 kilometers. Consequently, $\bar{\psi} = \bar{\psi}(\bar{h} = 200$ kilometers).

Figures 7 through 12 are plots of $\bar{\psi}(\bar{h} = 200)$ for the case in which $\Delta A = 0°$ and the values of initial longitude are ϕ_0 = 0°E, 60°E, 120°E, 180°, 120°W, and 60°W. Figures 13 through 18 are plots of $\bar{\psi}(\bar{h} = 200)$ for the same set of values of ϕ_0, with $\Delta A = -45°$. Figures 19 through 24 describe $\bar{\psi}(\bar{h} = 200)$ when $\Delta A = +45°$. Nadir angles of both 0° and 60° are evaluated in order to assess the dependence of $\bar{\psi}$ upon beam depression.

In the polar regions the azimuthal dependence of the radar beam is not too important, since $\theta \approx \chi$ implies that $H \cos\theta \sec\chi \approx H$. In the equatorial region, azimuthal and nadir angle variations are quite important. Consequently, a large variance in the amount of Faraday rotation may be expected to occur in the low and middle latitudes strictly on the basis of the predictable magnetic field parameter; in the polar region little variance is anticipated.

In order to estimate the amount of Faraday rotation which would typically be observed as a satellite orbits the earth, it is clear from Eq. 2 that some knowledge of the electron content is prerequisite. The most obvious way to invoke orbital dependence into the determination of the subsatellite content is to make use of ESSA charts of worldwide predictions of the routine ionospheric parameter MUF(zero)$F2$. According to simple Chapman theory, the content below the $F2$ maximum would be given by the product $\tau \cdot NF2$, where τ is some constant slab thickness. In reality, τ exhibits huge variations which may be uncorrelated with the variations in $NF2$. Since this approach is simple, it is unfortunate that it will lead to serious errors. The use of measured values of subsatellite content would be a more meaningful approach (8), but subsatellite content data for that portion of the ionosphere below the $F2$ maximum is sparse.

A Faraday rotation vhf-uhf polarization experiment (D-14) was conducted in conjunction with the Gemini IX spacecraft transits over Kauai, Hawaii, and Antigua, British West Indies. As of this writing it has been found that the subsatellite content over Hawaii varied between 3×10^{16} electrons/meter^2 following sunrise and 8×10^{16} electrons/meter^2* in the early afternoon. For all transits in which the experiment was conducted, the altitude of the spacecraft was h_s = 300 kilometers; consequently, the results approximately reflect the subpeak content. For a satellite orbiting at an altitude of 300 kilometers the subsatellite effective ionospheric slab thickness τ should never realistically exceed 100 kilometers. Furthermore, the maximum value of the plasma frequency f_p below the satellite is approximately 15 Mc/s. Since the content $C = \int N\, dh$ may be defined by the relation $C = 1.24 \times 10^{10} f_p{}^2 \tau$, it follows that $c \leq 2.8 \times 10^{17}\, m^{-2}$. Now the minimum value of τ

*Hereafter electrons/meter^2 will be abbreviated m^{-2}.

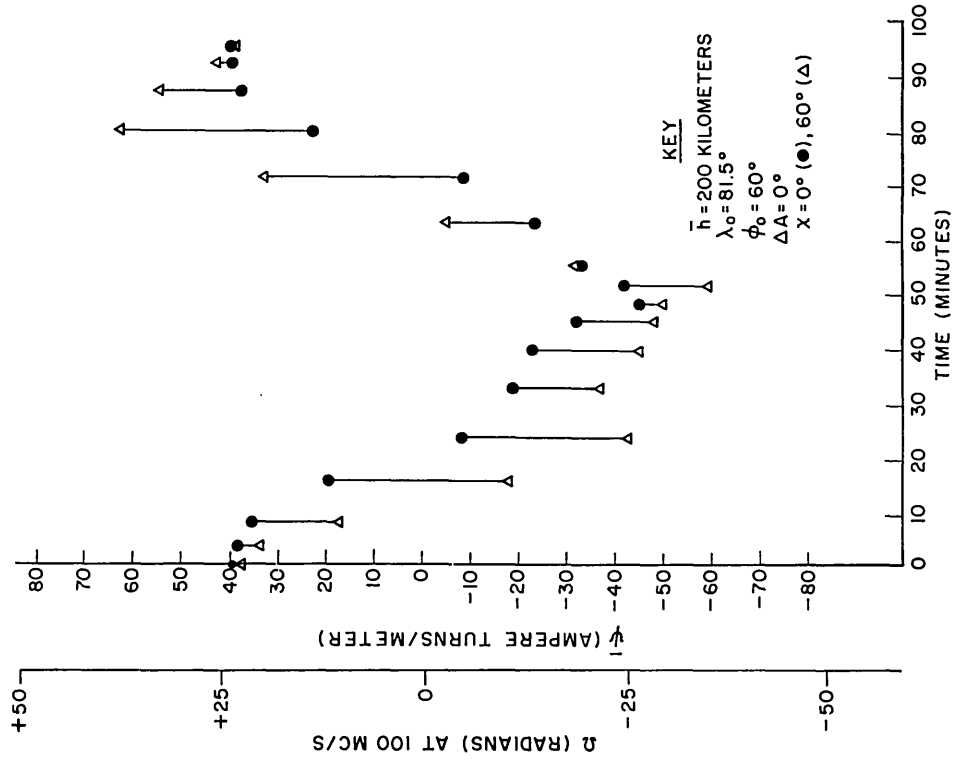

Fig. 8 - Magnetic field parameter, $\bar{\Psi}(\bar{h} = 200)$, and Faraday rotation, Ω (100 Mc/s), as functions of satellite time for $\phi_0 = 60°$ and $\Delta A = 0°$. The minus sign associated with ϕ_0 implies west longitude, and the positive sign implies east longitude. The horizontal orientation of the radar beam is defined by the azimuth function $A = A_v + \Delta A$ where all quantities are measured positive in the clockwise sense.

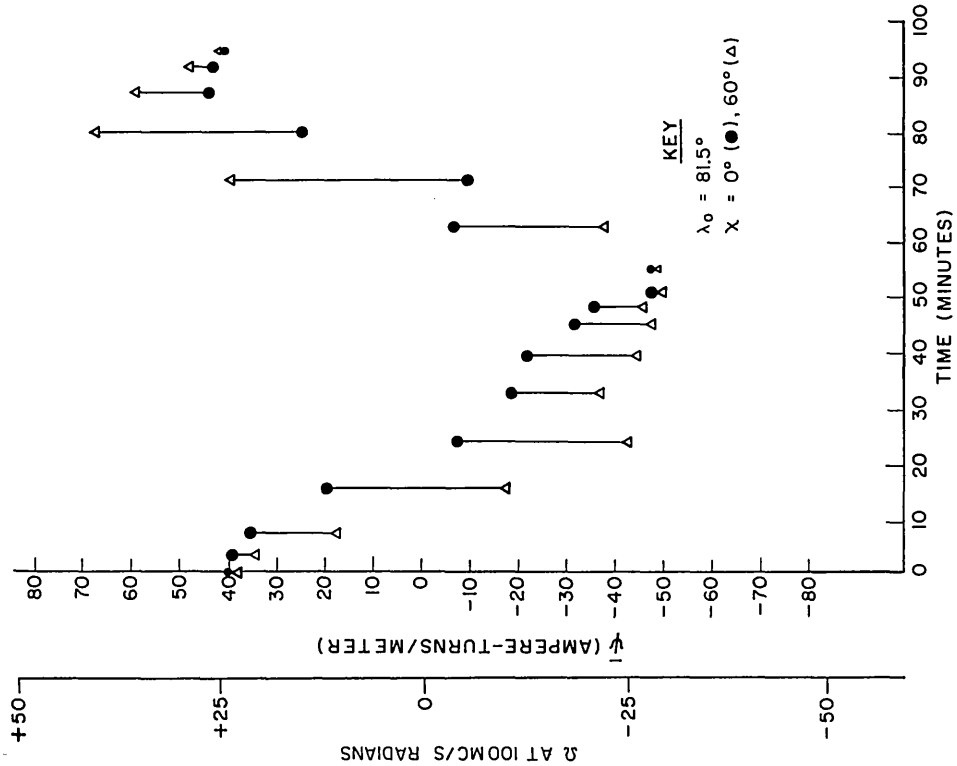

Fig. 7 - Magnetic field parameter, $\bar{\Psi}(\bar{h} = 200)$, and Faraday rotation, Ω (100 Mc/s), as functions of satellite time for $\phi_0 = 0°$ and $\Delta A = 0°$. The minus sign associated with ϕ_0 implies west longitude, and the positive sign implies east longitude. The horizontal orientation of the radar beam is defined by the azimuth function $A = A_v + \Delta A$ where all quantities are measured positive in the clockwise sense.

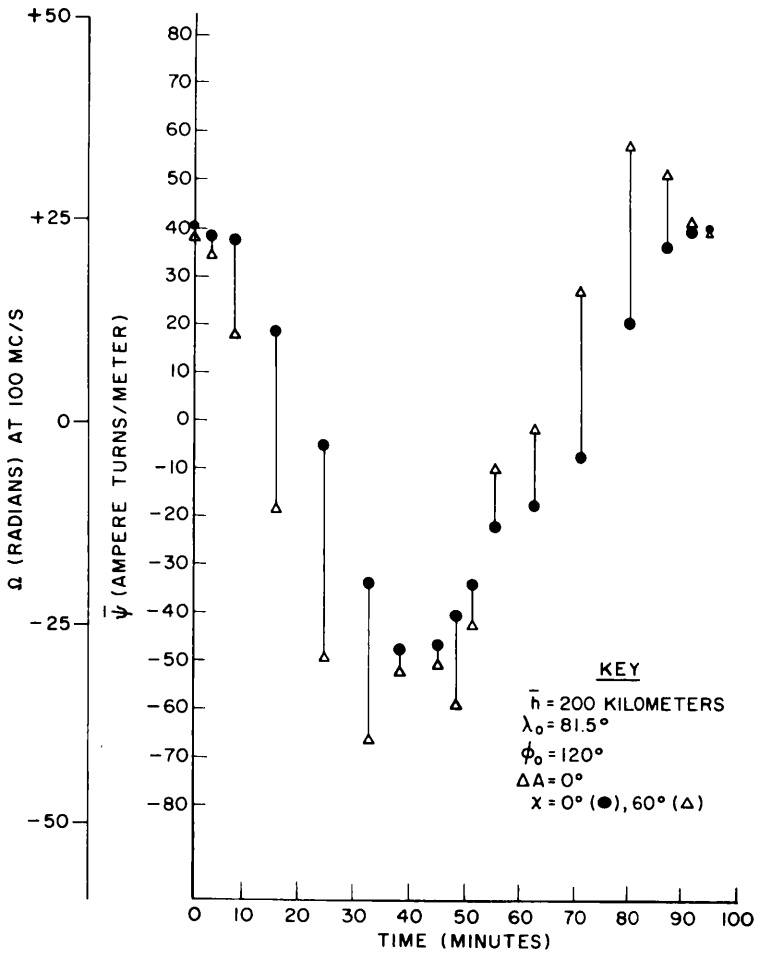

Fig. 9 - Magnetic field parameter, $\bar{\psi}(\bar{h} = 200)$, and Faraday rotation, Ω(100 Mc/s), as functions of satellite time for $\phi_0 = 120°$ and $\Delta A = 0°$. The minus sign associated with ϕ_0 implies west longitude, and the positive sign implies east longitude. The horizontal orientation of the radar beam is defined by the azimuth function $A = A_v + \Delta A$ where all quantities are measured positive in the clockwise sense.

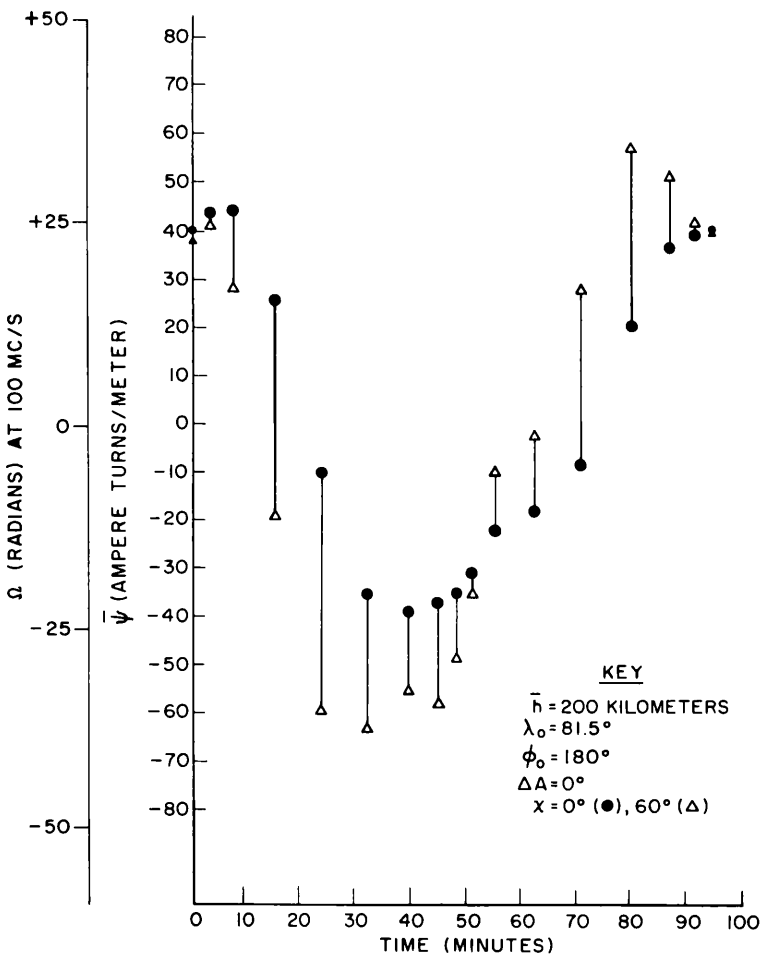

Fig. 10 - Magnetic field parameter, $\bar{\psi}(\bar{h} = 200)$, and Faraday rotation, Ω(100 Mc/s), as functions of satellite time for $\phi_0 = 180°$ and $\Delta A = 0°$. The minus sign associated with ϕ_0 implies west longitude, and the positive sign implies east longitude. The horizontal orientation of the radar beam is defined by the azimuth function $A = A_v + \Delta A$ where all quantities are measured positive in the clockwise sense.

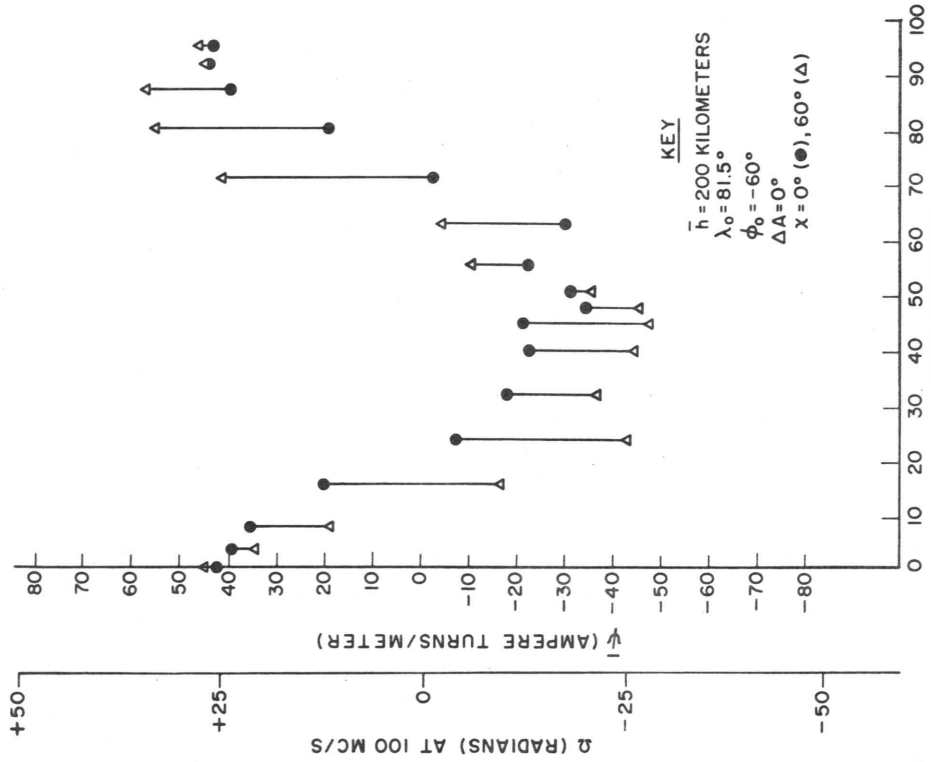

Fig. 12 - Magnetic field parameter, $\bar{\psi}(\bar{h} = 200)$, and Faraday rotation, Ω(100 Mc/s), as functions of satellite time for $\phi_0 = -60°$ and $\Delta A = 0°$. The minus sign associated with ϕ_0 implies west longitude, and the positive sign implies east longitude. The horizontal orientation of the radar beam is defined by the azimuth function $A = A_v + \Delta A$ where all quantities are measured positive in the clockwise sense.

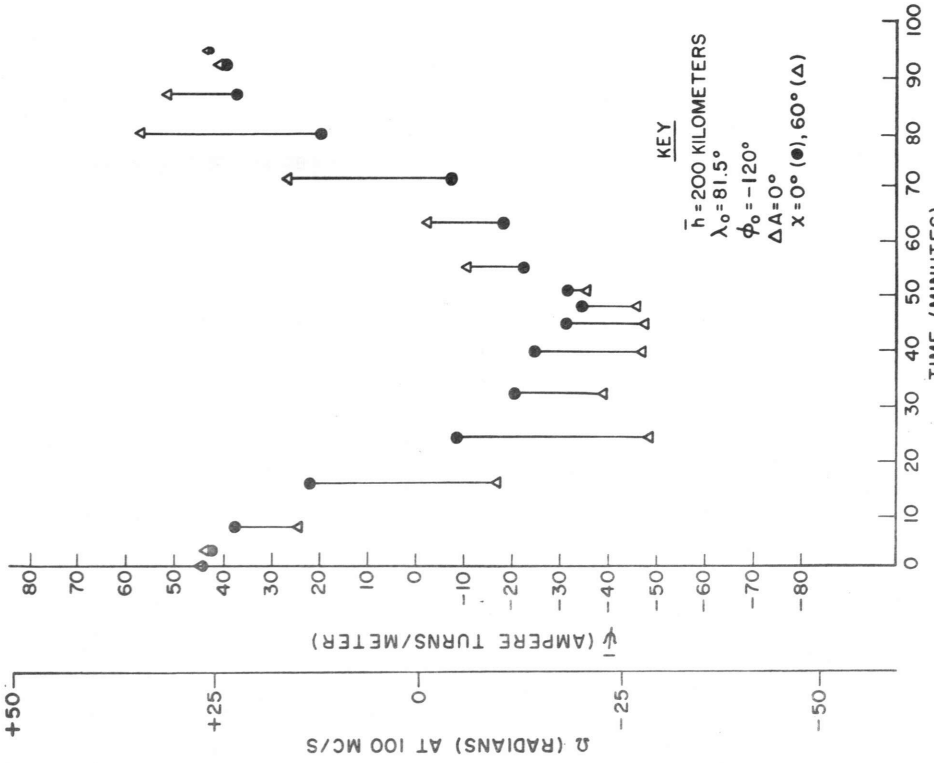

Fig. 11 - Magnetic field parameter, $\bar{\psi}(\bar{h} = 200)$, and Faraday rotation, Ω(100 Mc/s), as functions of satellite time for $\phi_0 = -120°$ and $\Delta A = 0°$. The minus sign associated with ϕ_0 implies west longitude, and the positive sign implies east longitude. The horizontal orientation of the radar beam is defined by the azimuth function $A = A_v + \Delta A$ where all quantities are measured positive in the clockwise sense.

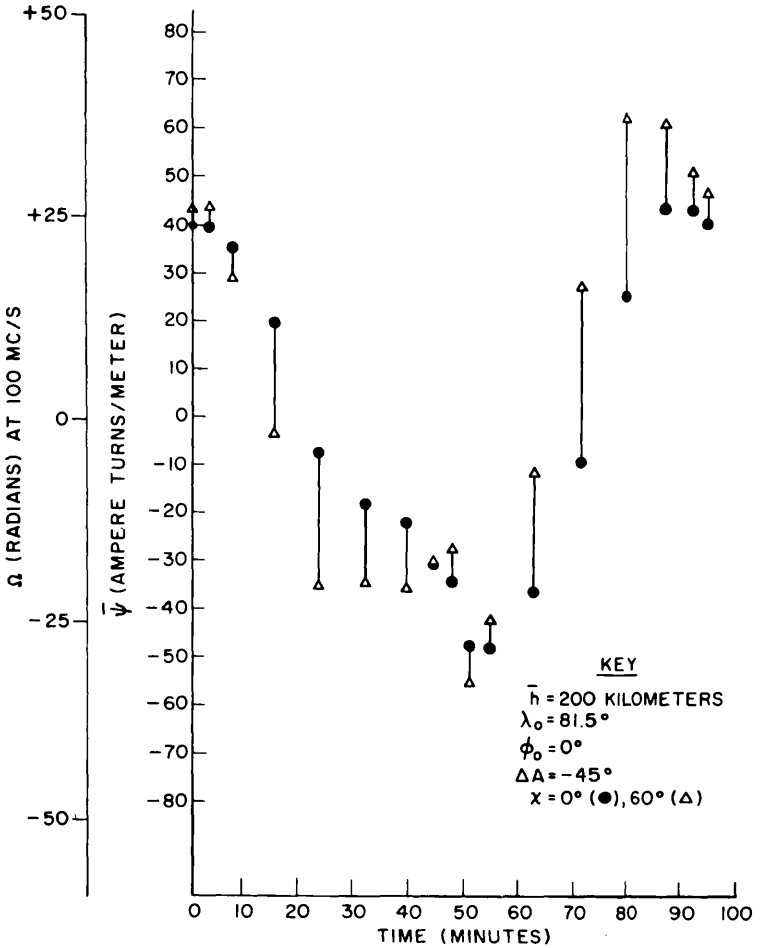

Fig. 13 - Magnetic field parameter, $\bar{\psi}(\bar{h} = 200)$, and Faraday rotation, Ω(100 Mc/s), as functions of satellite time for $\phi_0 = 0°$ and $\Delta A = -45°$. The minus sign associated with ϕ_0 implies west longitude, and the positive sign implies east longitude. The horizontal orientation of the radar beam is defined by the azimuth function $A = A_v + \Delta A$ where all quantities are measured positive in the clockwise sense.

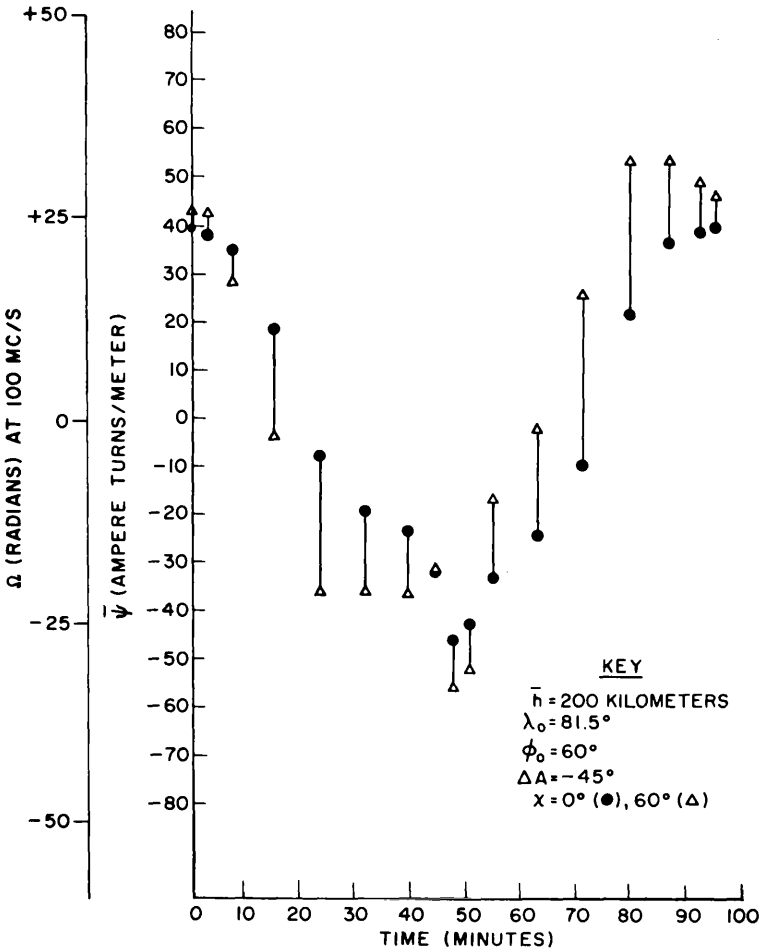

Fig. 14 - Magnetic field parameter, $\bar{\psi}(\bar{h} = 200)$, and Faraday rotation, Ω(100 Mc/s), as functions of satellite time for $\phi_0 = 60°$ and $\Delta A = -45°$. The minus sign associated with ϕ_0 implies west longitude, and the positive sign implies east longitude. The horizontal orientation of the radar beam is defined by the azimuth function $A = A_v + \Delta A$ where all quantities are measured positive in the clockwise sense.

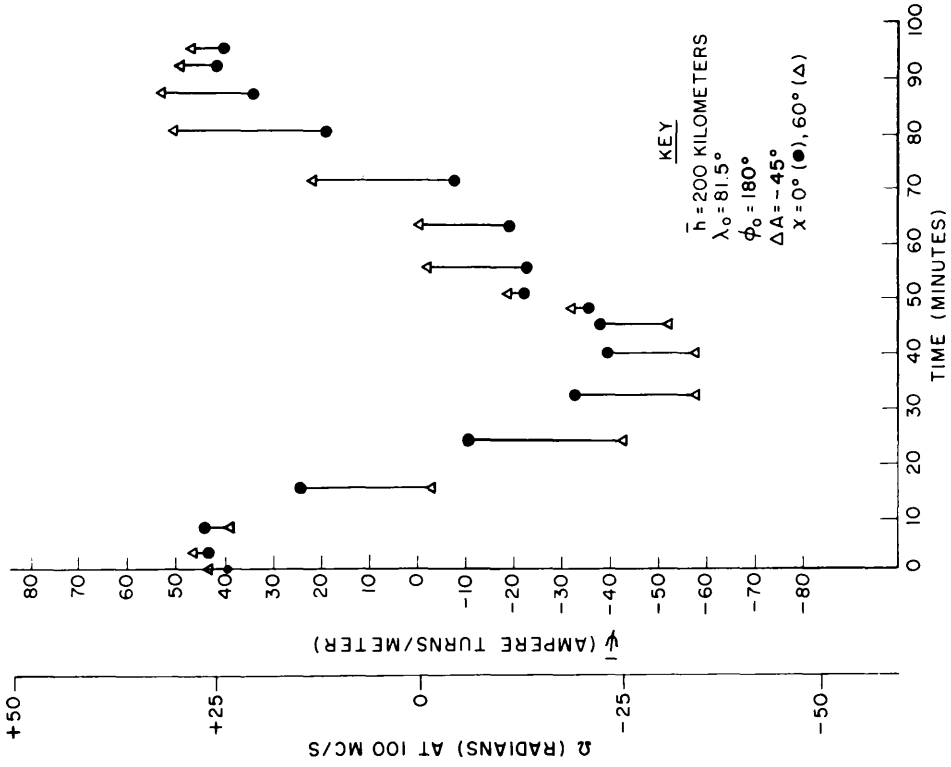

Fig. 16 - Magnetic field parameter, $\bar{\psi}(\bar{h} = 200)$, and Faraday rotation, $\Omega(100\ \mathrm{Mc/s})$, as functions of satellite time for $\phi_0 = 180°$ and $\Delta A = -45°$. The minus sign associated with ϕ_0 implies west longitude, and the positive sign implies east longitude. The horizontal orientation of the radar beam is defined by the azimuth function $A = A_v + \Delta A$ where all quantities are measured positive in the clockwise sense.

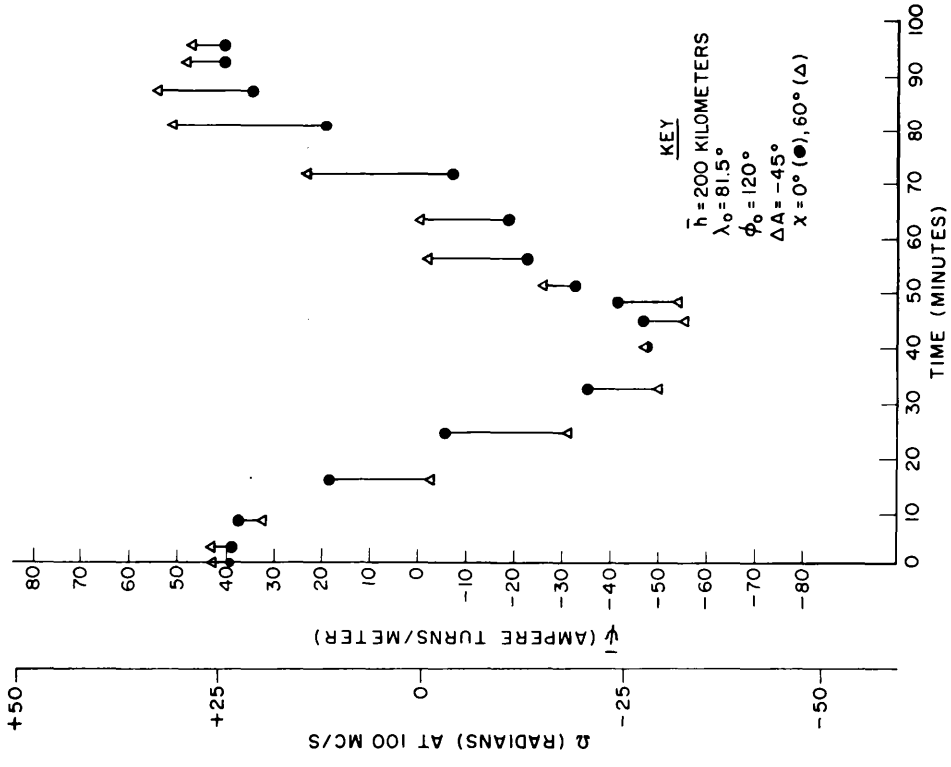

Fig. 15 - Magnetic field parameter, $\bar{\psi}(\bar{h} = 200)$, and Faraday rotation, $\Omega(100\ \mathrm{Mc/s})$, as functions of satellite time for $\phi_0 = 120°$ and $\Delta A = -45°$. The minus sign associated with ϕ_0 implies west longitude, and the positive sign implies east longitude. The horizontal orientation of the radar beam is defined by the azimuth function $A = A_v + \Delta A$ where all quantities are measured positive in the clockwise sense.

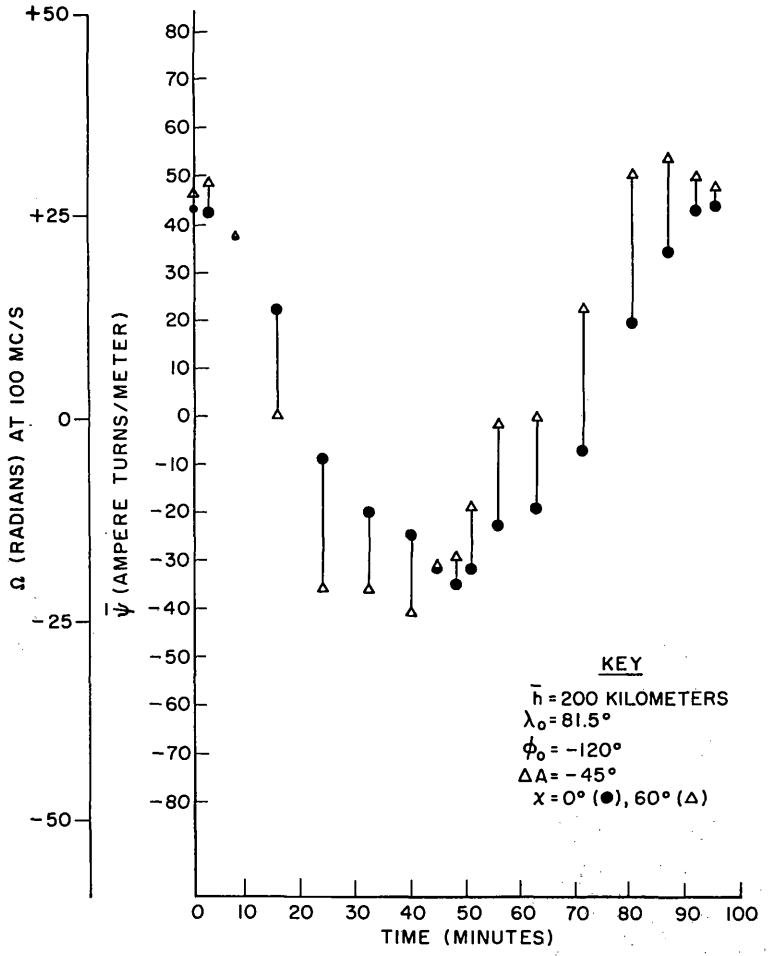

Fig. 17 - Magnetic field parameter, $\bar{\psi}(\bar{h} = 200)$, and Faraday rotation, Ω(100 Mc/s), as functions of satellite time for $\phi_0 = -120°$ and $\Delta A = -45°$. The minus sign associated with ϕ_0 implies west longitude, and the positive sign implies east longitude. The horizontal orientation of the radar beam is defined by the azimuth function $A = A_v + \Delta A$ where all quantities are measured positive in the clockwise sense.

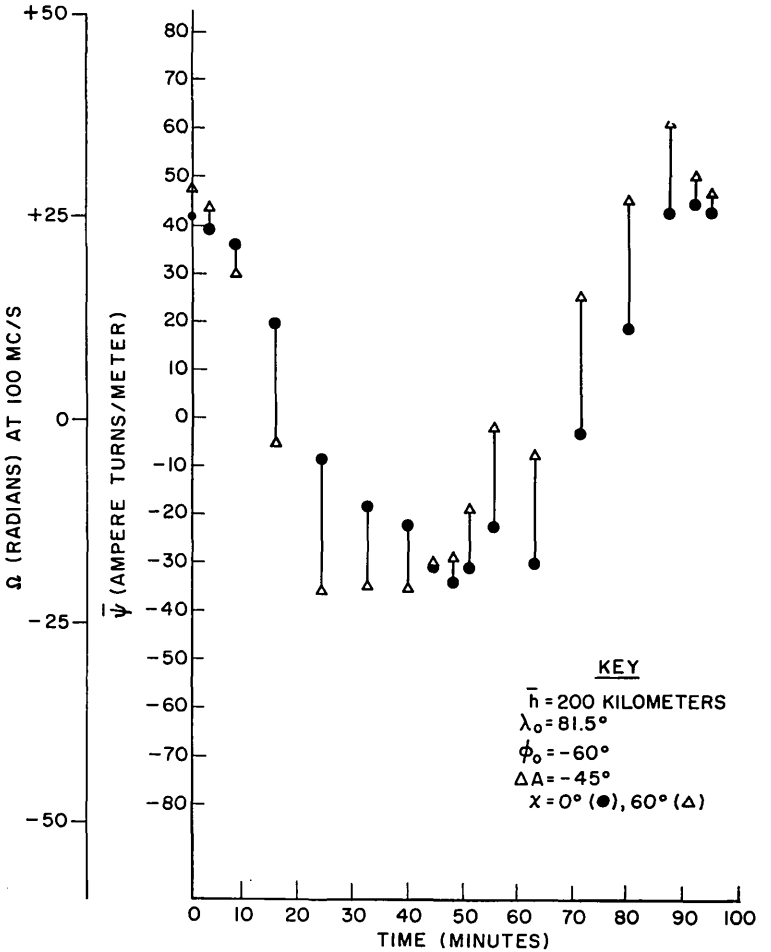

Fig. 18 - Magnetic field parameter, $\bar{\psi}(\bar{h} = 200)$, and Faraday rotation, Ω(100 Mc/s), as functions of satellite time for $\phi_0 = -60°$ and $\Delta A = -45°$. The minus sign associated with ϕ_0 implies west longitude, and the positive sign implies east longitude. The horizontal orientation of the radar beam is defined by the azimuth function $A = A_v + \Delta A$ where all quantities are measured positive in the clockwise sense.

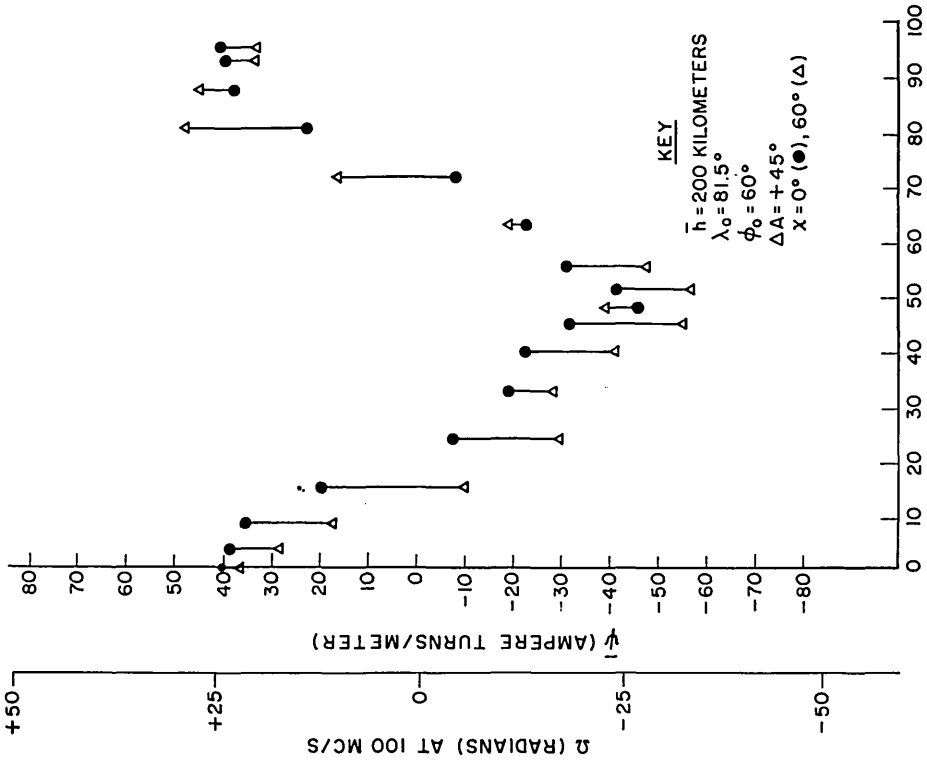

Fig. 20 - Magnetic field parameter, $\bar{\psi}(\bar{h} = 200)$, and Faraday rotation, $\Omega(100\ \mathrm{Mc/s})$, as functions of satellite time for $\phi_0 = 60°$ and $\Delta A = +45°$. The minus sign associated with ϕ_0 implies west longitude, and the positive sign implies east longitude. The horizontal orientation of the radar beam is defined by the azimuth function $A = A_v + \Delta A$ where all quantities are measured positive in the clockwise sense.

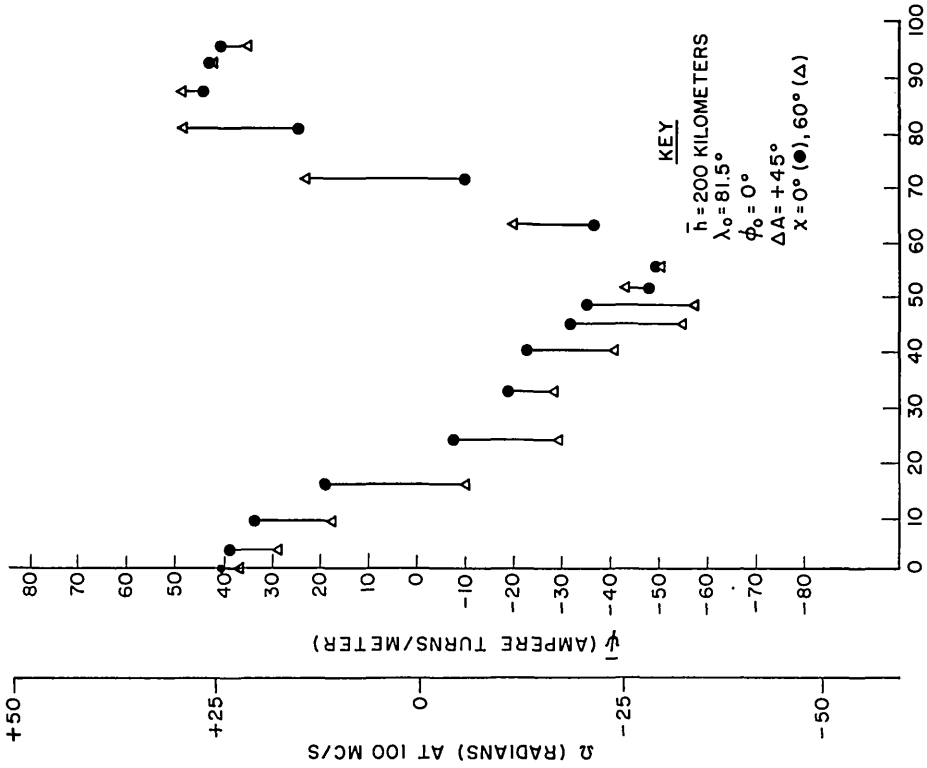

Fig. 19 - Magnetic field parameter, $\bar{\psi}(\bar{h} = 200)$, and Faraday rotation, $\Omega(100\ \mathrm{Mc/s})$, as functions of satellite time for $\phi_0 = 0°$ and $\Delta A = +45°$. The minus sign associated with ϕ_0 implies west longitude, and the positive sign implies east longitude. The horizontal orientation of the radar beam is defined by the azimuth function $A = A_v + \Delta A$ where all quantities are measured positive in the clockwise sense.

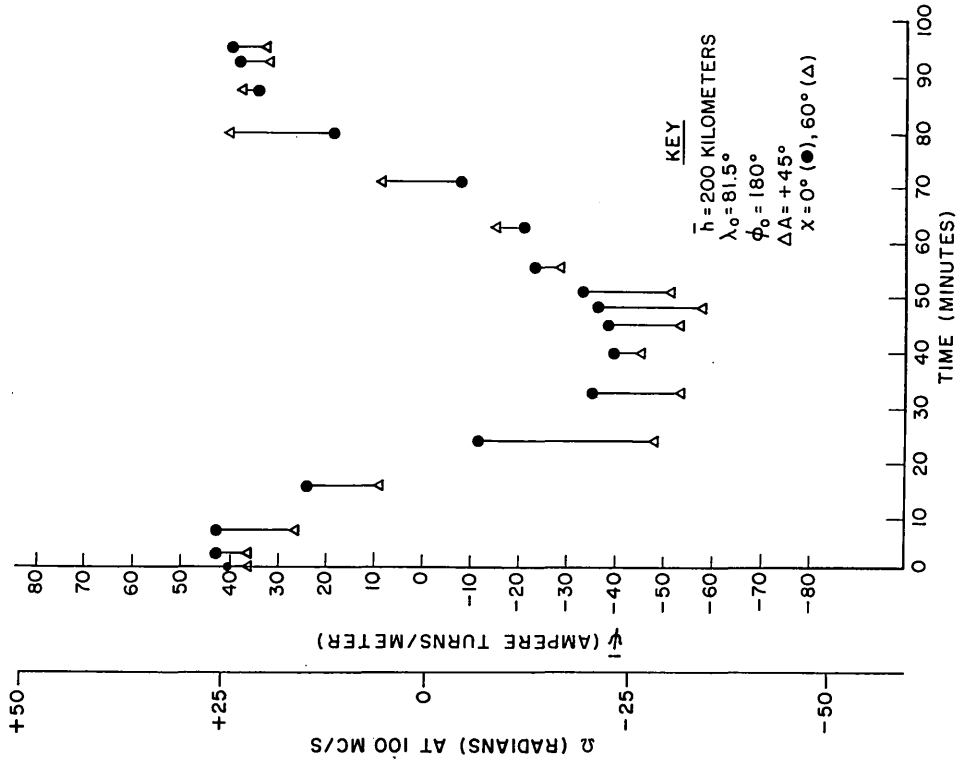

Fig. 22 - Magnetic field parameter, $\bar{\psi}(\bar{h} = 200)$, and Faraday rotation, Ω (100 Mc/s), as functions of satellite time for $\phi_0 = 180°$ and $\Delta A = +45°$. The minus sign associated with ϕ_0 implies west longitude, and the positive sign implies east longitude. The horizontal orientation of the radar beam is defined by the azimuth function $A = A_v + \Delta A$ where all quantities are measured positive in the clockwise sense.

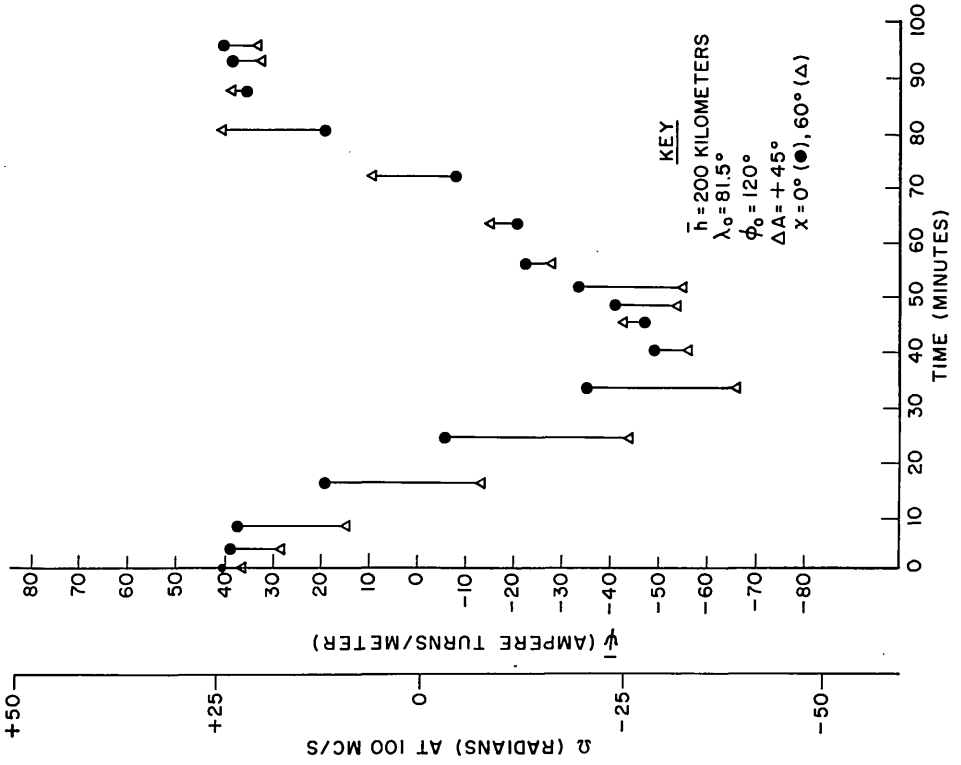

Fig. 21 - Magnetic field parameter, $\bar{\psi}(\bar{h} = 200)$, and Faraday rotation, Ω (100 Mc/s), as functions of satellite time for $\phi_0 = 120°$ and $\Delta A = +45°$. The minus sign associated with ϕ_0 implies west longitude, and the positive sign implies east longitude. The horizontal orientation of the radar beam is defined by the azimuth function $A = A_v + \Delta A$ where all quantities are measured positive in the clockwise sense.

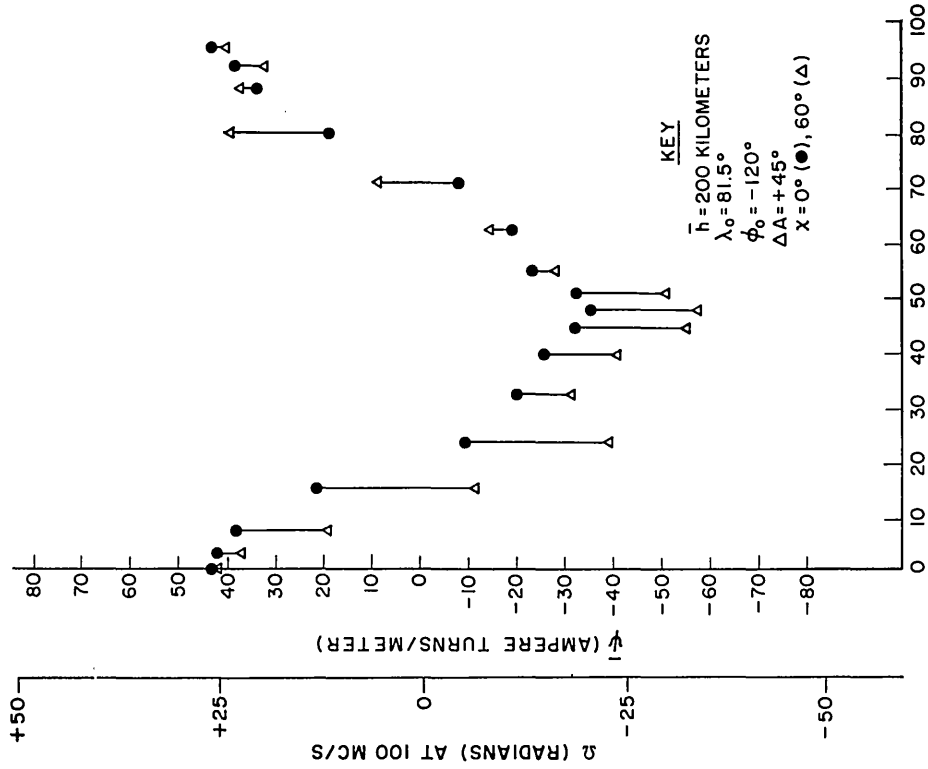

Fig. 23 - Magnetic field parameter, $\bar{\psi}(\bar{h} = 200)$, and Faraday rotation, Ω(100 Mc/s), as functions of satellite time for $\phi_0 = -120°$ and $\Delta A = +45°$. The minus sign associated with ϕ_0 implies west longitude, and the positive sign implies east longitude. The horizontal orientation of the radar beam is defined by the azimuth function $A = A_v + \Delta A$ where all quantities are measured positive in the clockwise sense.

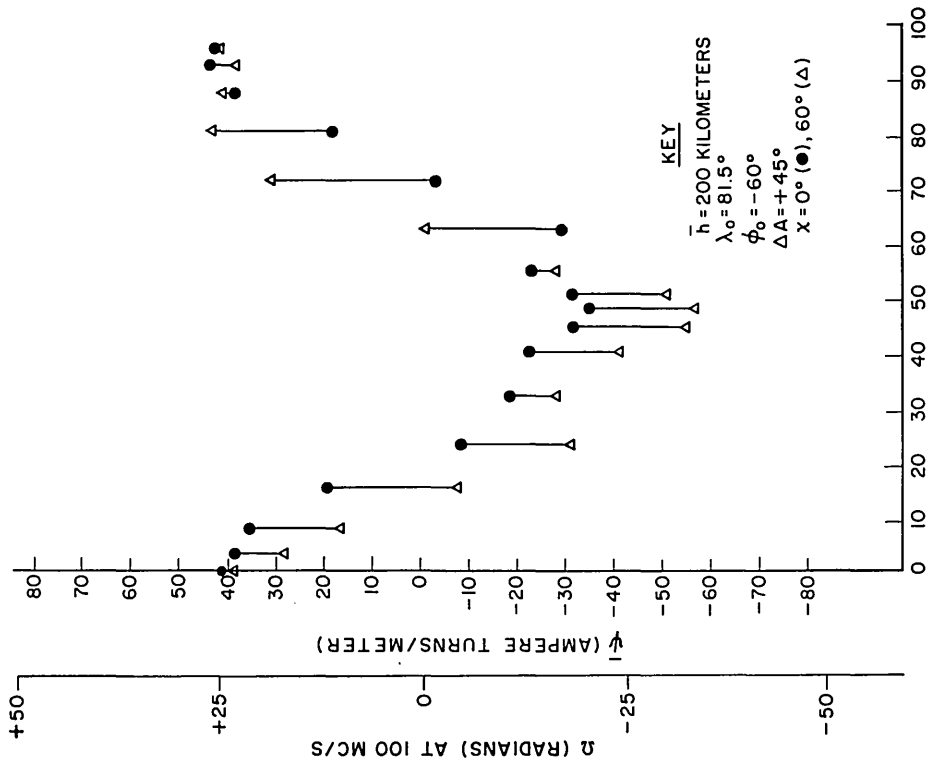

Fig. 24 - Magnetic field parameter, $\bar{\psi}(\bar{h} = 200)$, and Faraday rotation, Ω(100 Mc/s), as functions of satellite time for $\phi_0 = -60°$ and $\Delta A = +45°$. The minus sign associated with ϕ_0 implies west longitude, and the positive sign implies east longitude. The horizontal orientation of the radar beam is defined by the azimuth function $A = A_v + \Delta A$ where all quantities are measured positive in the clockwise sense.

is probably about 25 kilometers, and for a minimum plasma frequency of 2 Mc/s we find that $C \geq 1.2 \times 10^{15}\, m^{-2}$.

Figures 7 through 24 also depict the orbital variations of Faraday rotation at 100 Mc/s for the two-way radar case under the assumption that the subsatellite content C is $10^{17}\, m^{-2}$. (It is implicit that the limits of integration are between the satellite radar altitude of 300 kilometers and the altitude of the "base" of the ionosphere $\approx$ 90 kilometers.) It is noteworthy that under these conditions the absolute value of the 100 Mc/s Faraday rotation, $|\Omega$ (100 Mc/s)$|$, is characteristically less than 50 radians or 8 complete rotations. Therefore, it may be stated with reasonable assurance that the total excursion in the Faraday rotation between adjacent orbital extrema, i.e., $|\Delta\Omega$ (100 Mc/s)$|$, should be no greater than 16 rotations, and a linearly polarized receiver channel should exhibit fewer than 32 fades.* Since $\Omega \propto f^{-2}$, it follows that $|\Delta\Omega$ (1000 Mc/s)$|$ should not exceed 0.16 rotation or 0.32 of a complete fade. During an entire orbital period Ω(1000 Mc/s) should not exceed 1/2 radian in either the clockwise or counterclockwise sense provided $C \approx 10^{17}\, m^{-2}$. Taking the transmitter and receiver polarizations to be linear and having the same orientation, we would not expect the signal degradation due to Faraday rotation A_F to exceed 2 dB at 1000 Mc/s.

In order to compare the amounts of Faraday rotation degradation A_F (in decibels) which might be anticipated as a function of the time of day, season, and sunspot number, R_z, a constant value $\bar{\psi}$ = 40 ampere-turns/meter has been assumed as well as certain values of content which are felt to represent the average lower ionosphere under various conditions. The assumed values of content are listed in Table 1, and the computed values of A_F are given in Table 2. Upon inspection of Table 2, we see that $|A_F|$ is less than 2 dB for a radar frequency of 1000 Mc/s regardless of conditions. With the exception of winter days during high solar activity $|A_F|$ is less than 2 dB at 800 Mc/s. It is also noteworthy that $|A_F|$ is less than 2 dB for all radar frequencies above 100 Mc/s during winter nights in which solar activity is low. It is emphasized that Table 2 should not be interpreted rigidly inasmuch as the ionospheric electron content always exhibits a more or less unpredictable variance.

Table 1
Electron Content of the Ionosphere
Below 300 Kilometers*

Time of Day	Electron Content (10^{17} electrons/m^2)	
	High R_z	Low R_z
Wintertime		
Day	2.5	0.25
Night	0.25	0.025
Summertime		
Day	1.35	0.40
Night	0.135	0.040

*Values assumed for computations of A_F.

*A fade is defined to be a polarization shift of π radians.

Table 2
Signal Degradation Due to Faraday Rotation A_F

Faraday Rotation A_F	Signal Degradation* (dB)			
	Day		Night	
	High R_z	Low R_z	High R_z	Low R_z
Wintertime				
1000†	-1.63	- 0.02	- 0.02	≈0
800	-4.46	- 0.04	- 0.04	≈0
600	-∞	- 0.12	- 0.12	≈0
400	-∞	- 0.61	- 0.61	≈0
200	-∞	-21.46	-21.46	-0.10
100	-∞	-∞	-∞	-1.63
Summertime				
1000	-0.45	- 0.04	≈ 0	≈0
800	-1.14	- 0.10	- 0.01	≈0
600	-4.02	- 0.31	- 0.03	≈0
400	-∞	- 1.62	- 0.18	-0.02
200	-∞	-∞	- 3.00	-0.25
100	-∞	-∞	-∞	-4.10

*The value of $A_F = -\infty$ implies that the Faraday rotation is at least as great as 90°.
†Frequency designation in Mc/s.

Without an a priori specification of the radar beam orientation, we may determine a number $\overline{H \csc I}$ which is no less than one-half the maximum value of $\bar{\psi}$ which may occur at a particular latitude and longitude. Having $\overline{H \csc I}$ at our disposal, we are able to compute the Faraday rotation which corresponds to at least one-half the maximum amount quite easily. The rotation angle corresponding to $\overline{H \csc I}$ (denoted by the symbol $\tilde{\Omega}$) is related to the maximum rotation angle Ω_{max} by

$$\Omega_{max} = \left[\frac{(\overline{H \cos\theta \sec\chi})_{max}}{\overline{H \csc I}}\right] \tilde{\Omega}. \tag{6}$$

The ratio of $(\overline{H \cos\theta \sec\chi})_{max}$ to $\overline{H \csc I}$ is given in Fig. 25 as a function of θ with I as parameter. In order to maximize $\overline{\cos\theta \sec\chi}$ we require that the radio path have an orientation with respect to geographic north such that the radar beam azimuth is given by $A = D \pm n \cdot 180°$ ($n = 0,1$), where D is the magnetic declination and n is chosen to render the largest value of $\cos\theta$. Given the magnetic inclination I, it follows that for any value of θ there exist two values of the beam nadir angle (e.g., χ_1 and χ_2). We therefore choose θ (χ) such that χ equals the maximum value of χ_1 and χ_2, which automatically maximizes $\sec\chi$. In order to restrict the beam depression angles of the radio path to meaningful values (to see the horizon from an altitude of 300 kilometers, the beam must be depressed at least 17 degrees from the horizontal) it is further assumed that $\theta \leq I - 20°$. Near the magnetic equator the relationship between $\overline{H \csc I}$ and $(\overline{H \cos\theta \sec\chi})_{max}$ breaks down, since $\overline{H \csc I} \to \infty$ as $I \to 0$. It may be shown that the function $\overline{H \tan\chi}$ is a measure of $(\overline{H \cos\theta \sec\chi})_{max}$ near the magnetic equator. Clearly, a vertically directed radar beam will exhibit no Faraday rotation at the magnetic equator. This is seen from Figs. 8 through 24. The function $\overline{H \csc I}$ has been computed for latitudes of ±75°, ±60°, ±45°, ±30°, ±15°, and 0° corresponding to each of the following longitudes: 0° (Greenwich), ±15°, ±30°, ±45°, ±60°,

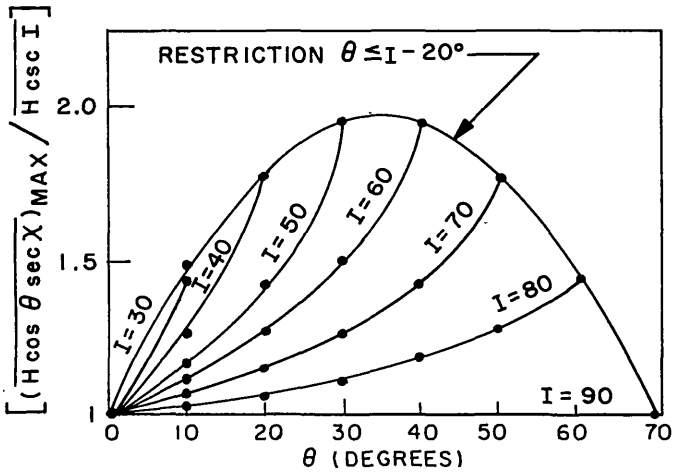

Fig. 25 - Ratio of $(\overline{H \cos\theta \sec\chi})_{max}$ to $\overline{H \csc I}$ as a function of θ with I as parameter. The maximum value of $\overline{H \cos\theta \sec\chi}$ is no longer approximated by $\overline{H \csc I}$ (even within a predictable factor of two) as $I \to 0°$, since $\overline{H \csc I}$ becomes infinite. Therefore the ratio is undefined near the magnetic equator.

±75°, ±90°, ±105°, ±120°, ±135°, ±150°, ±165°, and 180°. Figures 26 through 32 are charts of $\overline{H \csc I}$ as well as $\tilde{\Omega}$(100 Mc/s), $\tilde{\Omega}$(200 Mc/s), $\tilde{\Omega}$(400 Mc/s), $\tilde{\Omega}$(600 Mc/s), $\tilde{\Omega}$(800 Mc/s), and $\tilde{\Omega}$(1000 Mc/s) under the assumption that $C = 10^{17}\, m^{-2}$. The magnetic field intensity H increases toward the poles and $\csc I$ decreases toward the poles; as a result, $\overline{H \csc I}$ is relatively constant on a worldwide basis. (Values of $\overline{H \csc I}$ and the rotation angles to which it corresponds have been deleted from Figures 26 through 32 near the magnetic equator, since in that region the quantity $\overline{H \csc I}$ is unrelated to the maximum value of $\overline{H \cos\theta \sec\chi}$ under the constraint that the beam depression angle $90° - \chi \geq 20°$.) We see from Fig. 27 that $\tilde{\Omega}$(100 Mc/s) is characteristically less than 30 radians. This is in agreement with the conclusion drawn from Figs. 7 through 24 in which Ω(100 Mc/s) never exceeded 50 radians.

The curves of Ω(100 Mc/s)—Figs. 7 through 24 suggest the Faraday fade rates to be expected as a satellite orbits the earth. These rates are largely fictitious, however, since they are referenced to a moving reference point. These figures are primarily useful because they imply the relative amount of Faraday rotation to be expected upon acquisition of a target for a fixed beam orientation. The charts of $\tilde{\Omega}$ yield information as to the maximum rotation to be expected as a function of radar frequency and satellite position.

Case 2 - Fixed Reference Point

The amount of rotation for the fixed reference point case is limited by the results of the preceding section concerning the moving reference point. An additional feature for this case is the determination of the number of fades which a returned radar signal undergoes as a function of time.

Figure 33 is a plot of $\bar{\psi}(\bar{h} = 200)$ for the Randle Cliff Radar site near Chesapeake Beach, Maryland. If we restrict the earth-radar elevation angle ϵ to angles in excess of 20°, it is equivalent to restricting the satellite-radar beam nadir angle χ to angles less than 70°, since $\chi = 90° - \epsilon$. Under these conditions we see that $\bar{\psi}(\bar{h} = 200)$ varies between

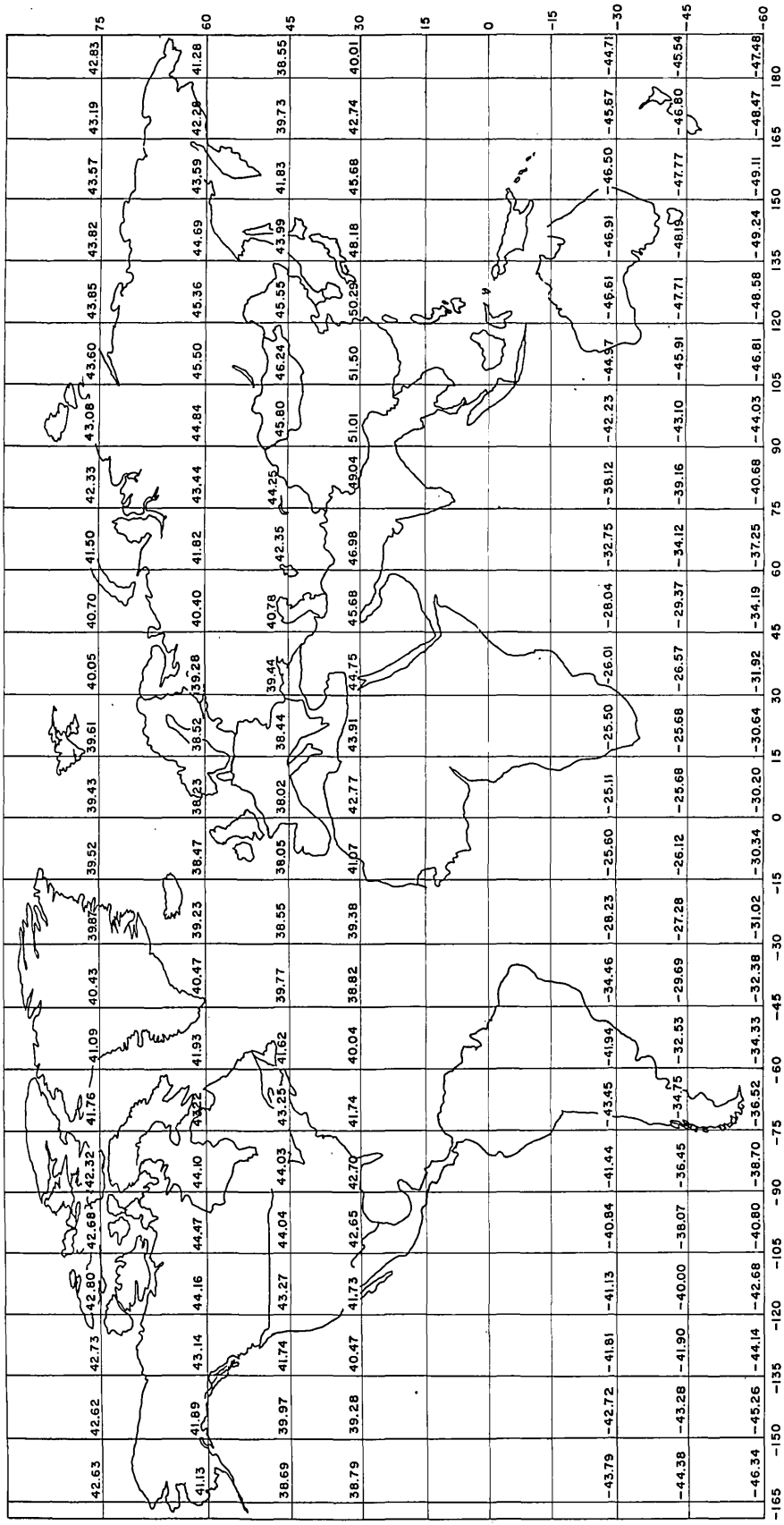

Fig. 26 - Values of $\overline{H \csc I}$ which are ≥ twice the maximum values of the magnetic field parameter $(\overline{H \cos\theta \sec\chi})_{max}$ (Note: $H \cos\theta \sec\chi \rightarrow H \csc I$ when $\theta = 0°$ and $\chi = 90° - I$). H is the magnetic field intensity in ampere-turns/meter, θ is the propagation angle, χ is the beam depression angle, and I is the magnetic field inclination angle. The abscissa is geographic longitude with respect to Greenwich (in degrees) and the ordinate is geographic latitude (in degrees). $(\overline{H \cos\theta \sec\chi})_{max}$ is not related to $\overline{H \csc I}$ near the magnetic equator. Hence, values of $\overline{H \csc I}$ between ±15° geographic latitude have been deleted from the chart.

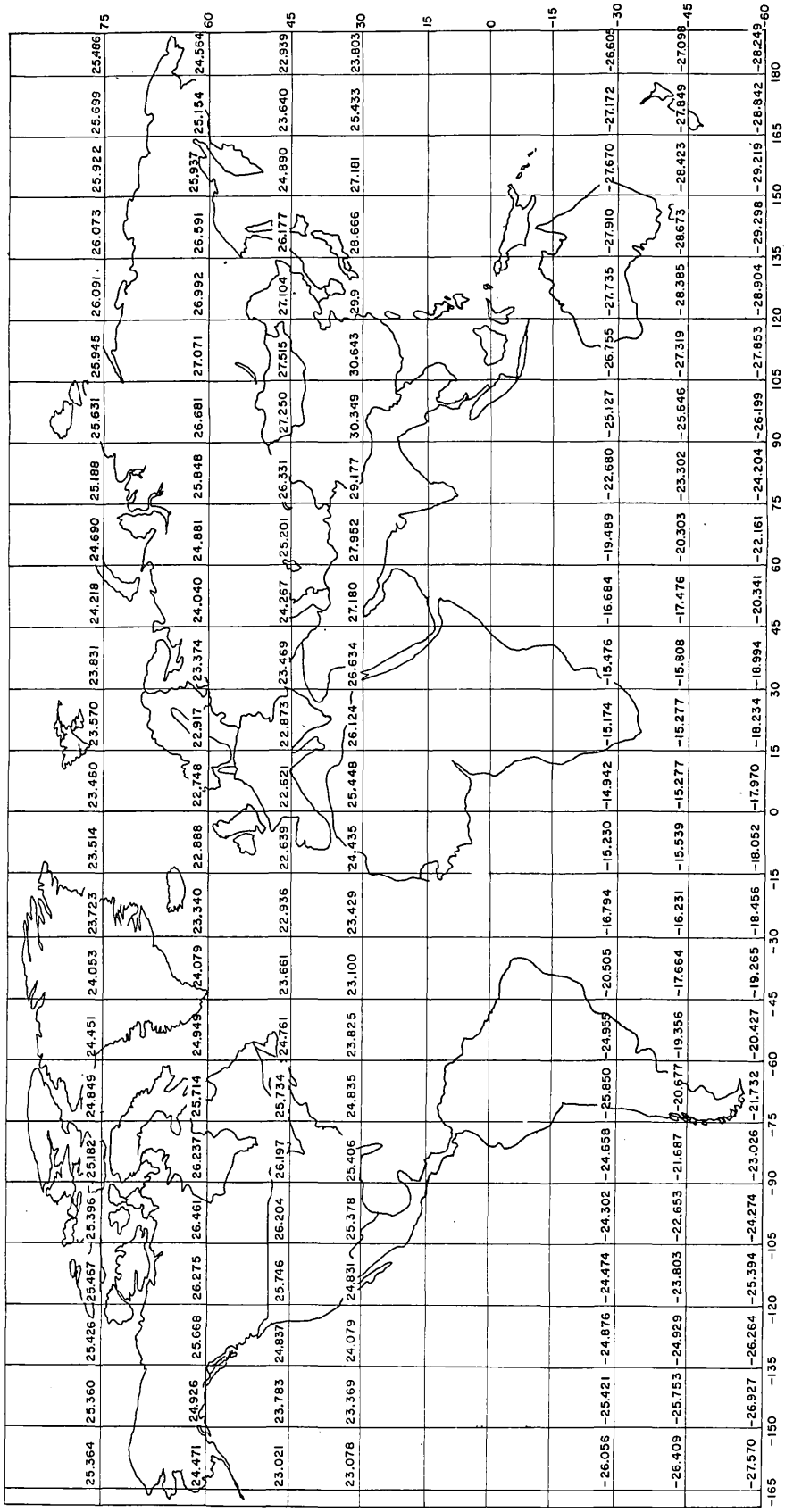

Fig. 27 - Values of the Faraday rotation, $\tilde{\Omega}$ (100 Mc/s), which corresponds to at least one-half the maximum possible amount. Computations are based upon the values of $\overline{H \csc I}$ given in Fig. 26 and for $C = 10^{17}$ m^{-2}. The abscissa is geographic longitude (degrees) and the ordinate is geographic latitude (degrees). The values of $\tilde{\Omega}$ are in radians.

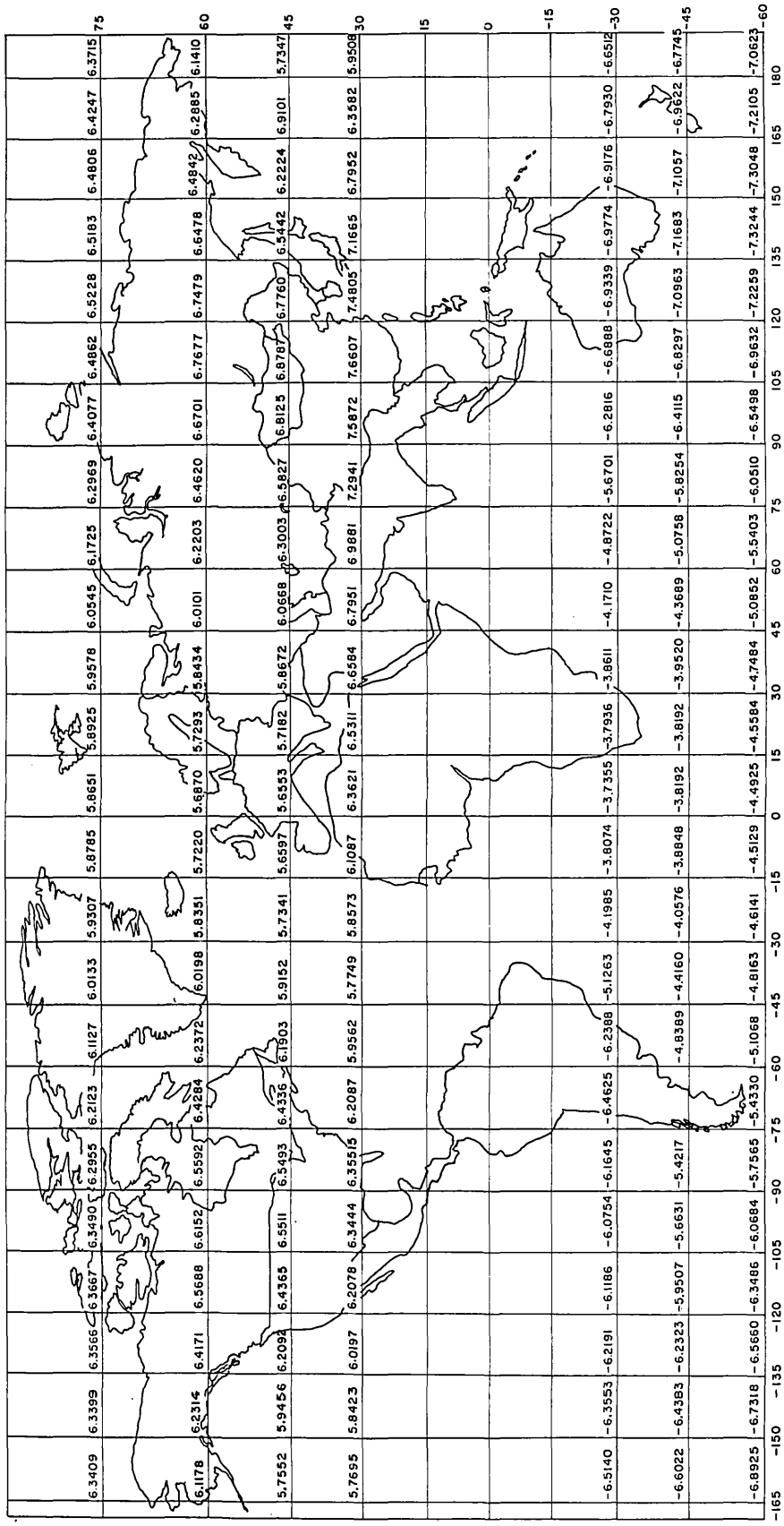

Fig. 28 - Values of the Faraday rotation, $\tilde{\Omega}$(200 Mc/s), which corresponds to at least one-half the maximum possible amount. Computations are based upon the values of $H \csc I$ given in Fig. 26 and for $C = 10^{17}$ m^{-2}. The abscissa is geographic longitude (degrees) and the ordinate is geographic latitude (degrees). The values of Ω are in radians.

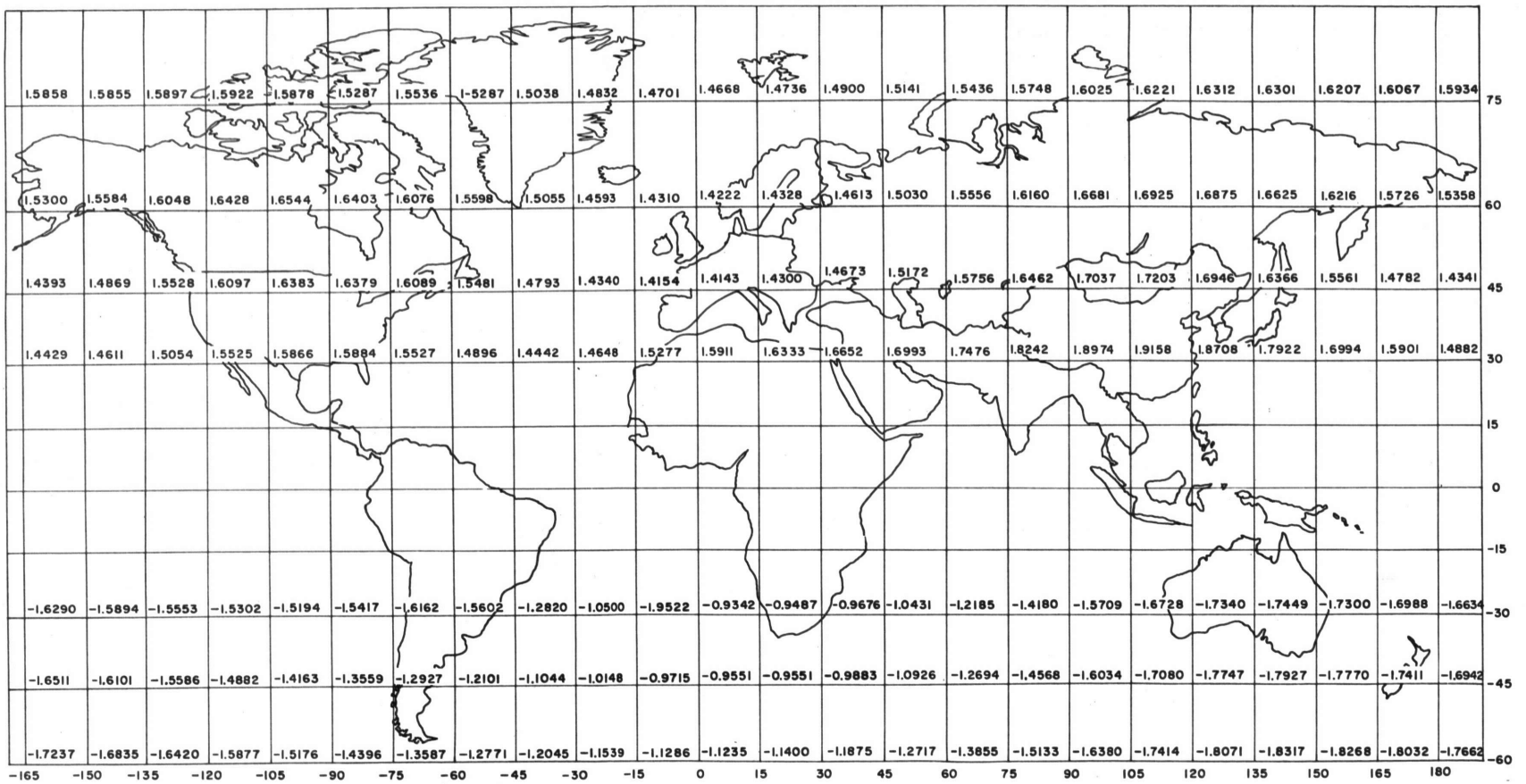

Fig. 29 - Values of the Faraday rotation, $\tilde{\Omega}$(400 Mc/s), which corresponds to at least one-half the maximum possible amount. Computations are based upon the values of $\overline{H} \csc \overline{I}$ given in Fig. 26 and for $C = 10^{17}$ m^{-2}. The abscissa is geographic longitude (degrees) and the ordinate is geographic latitude (degrees). The values of Ω are in radians.

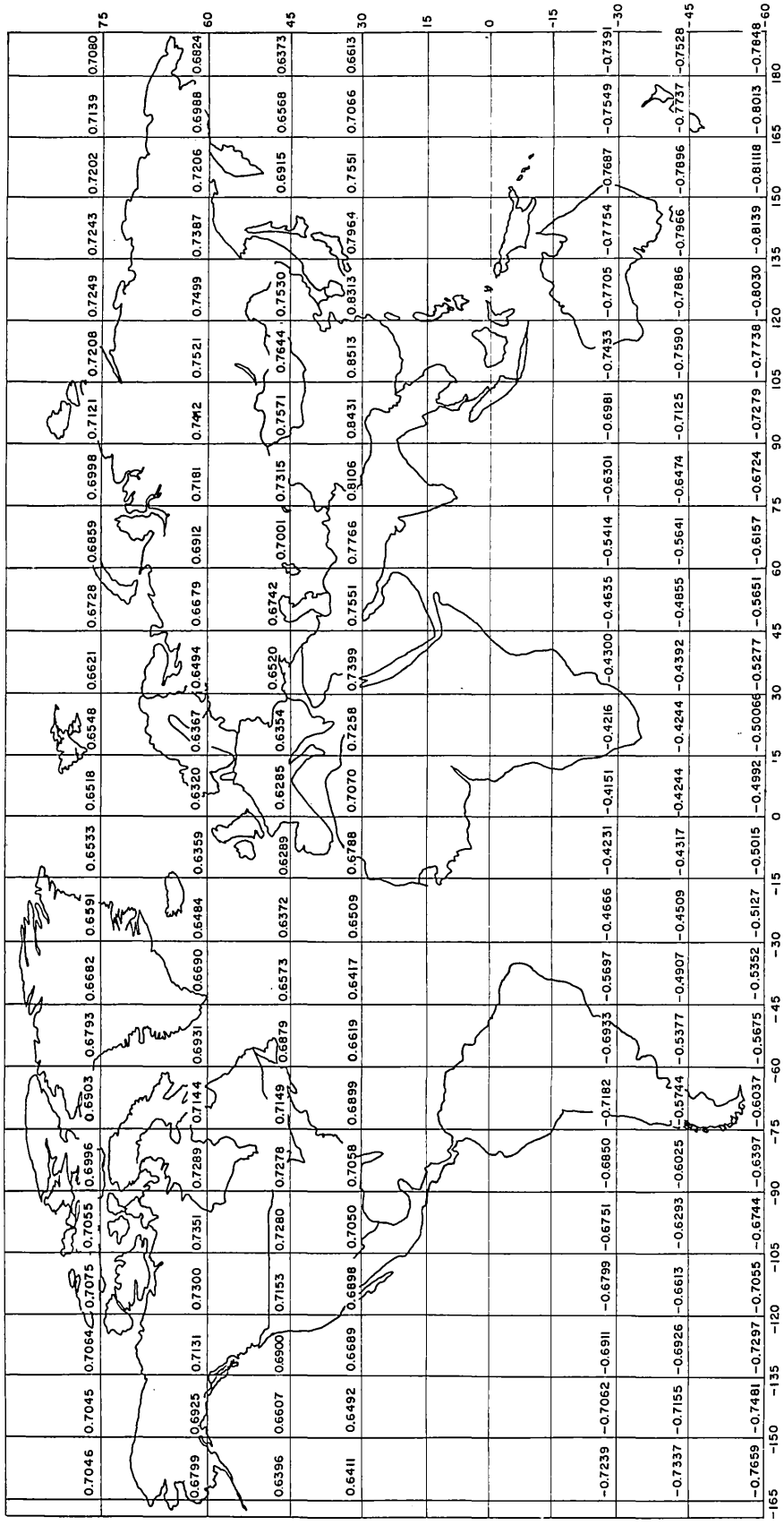

Fig. 30 - Values of the Faraday rotation, $\tilde{\Omega}$(600 Mc/s), which corresponds to at least one-half the maximum possible amount. Computations are based upon the values of $\overline{H}$ csc $\overline{I}$ given in Fig. 26 and for $C = 10^{17}$ m^{-2}. The abscissa is geographic longitude (degrees) and the ordinate is geographic latitude (degrees). The values of Ω are in radians.

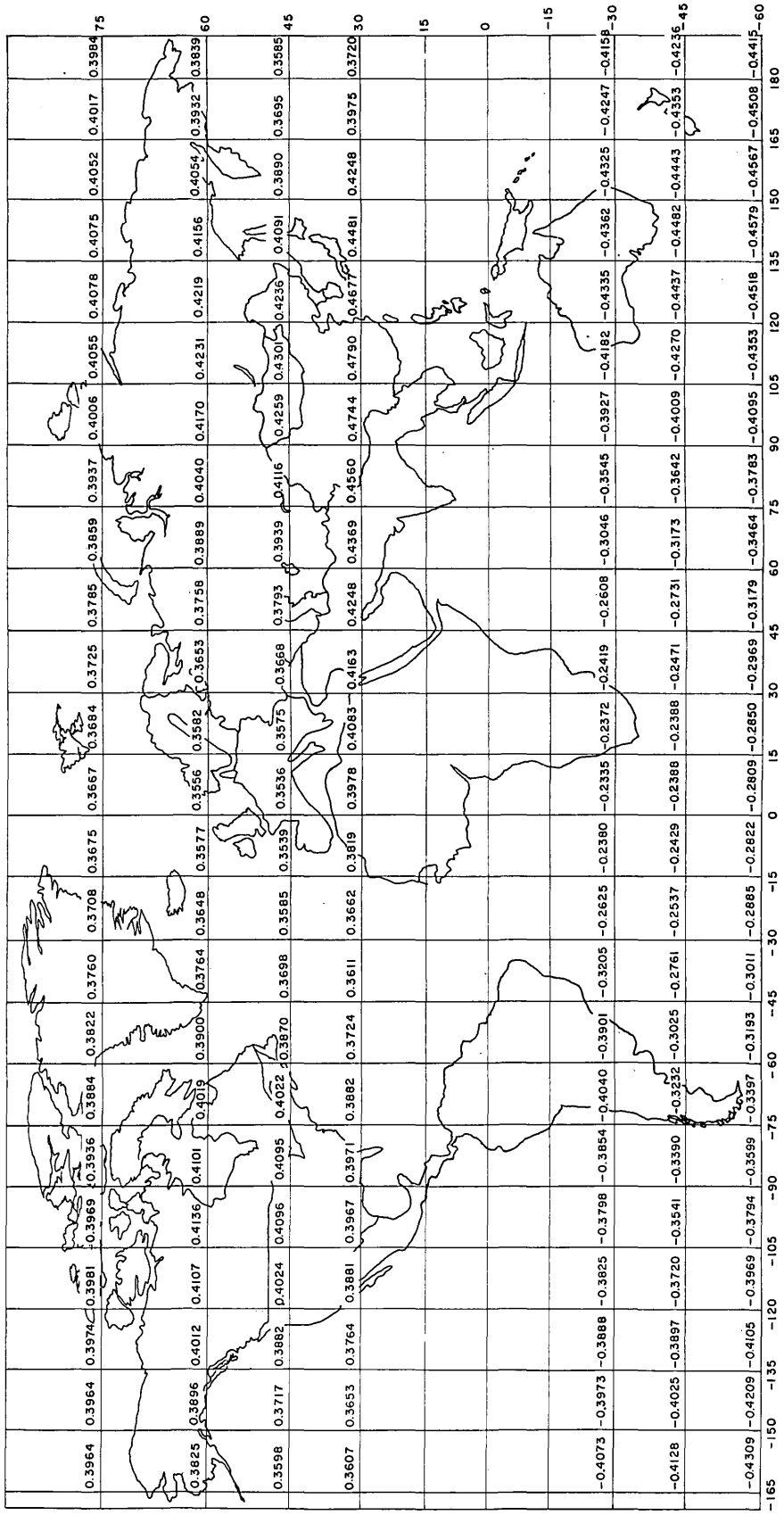

Fig. 31 - Values of the Faraday rotation, $\tilde{\Omega}$ (800 Mc/s), which corresponds to at least one-half the maximum possible amount. Computations are based upon the values of $\overline{H \csc I}$ given in Fig. 26 and for $C = 10^{17}$ m^{-2}. The abscissa is geographic longitude (degrees) and the ordinate is geographic latitude (degrees). The values of Ω are in radians.

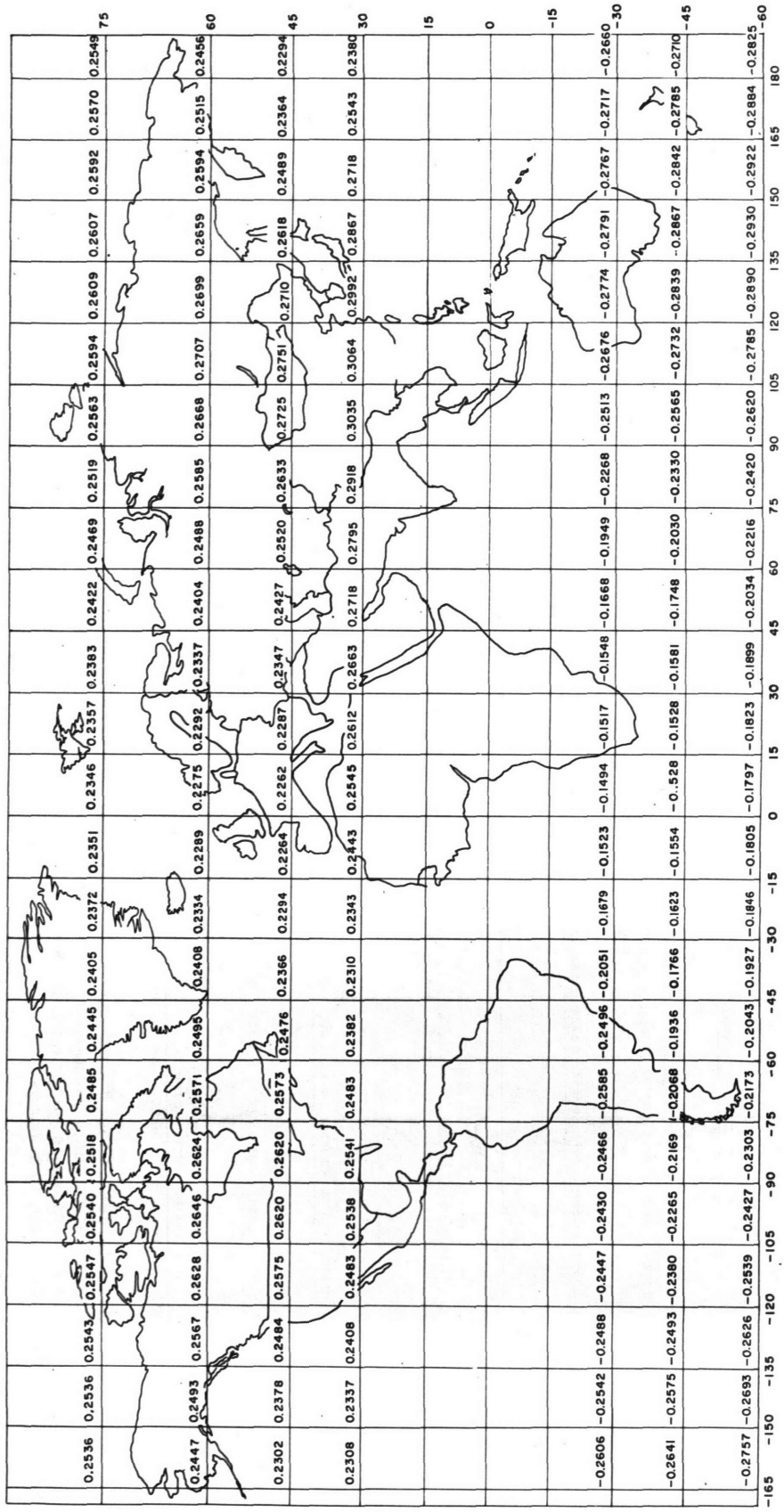

Fig. 32 - Values of the Faraday rotation, $\tilde{\Omega}$(1000 Mc/s), which corresponds to at least one-half the maximum possible amount. Computations are based upon the values of $\overline{H}\csc\overline{I}$ given in Fig. 26 and for $C = 10^{17}$ m^{-2}. The abscissa is geographic longitude (degrees) and the ordinate is geographic latitude (degrees). The values of Ω are in radians.

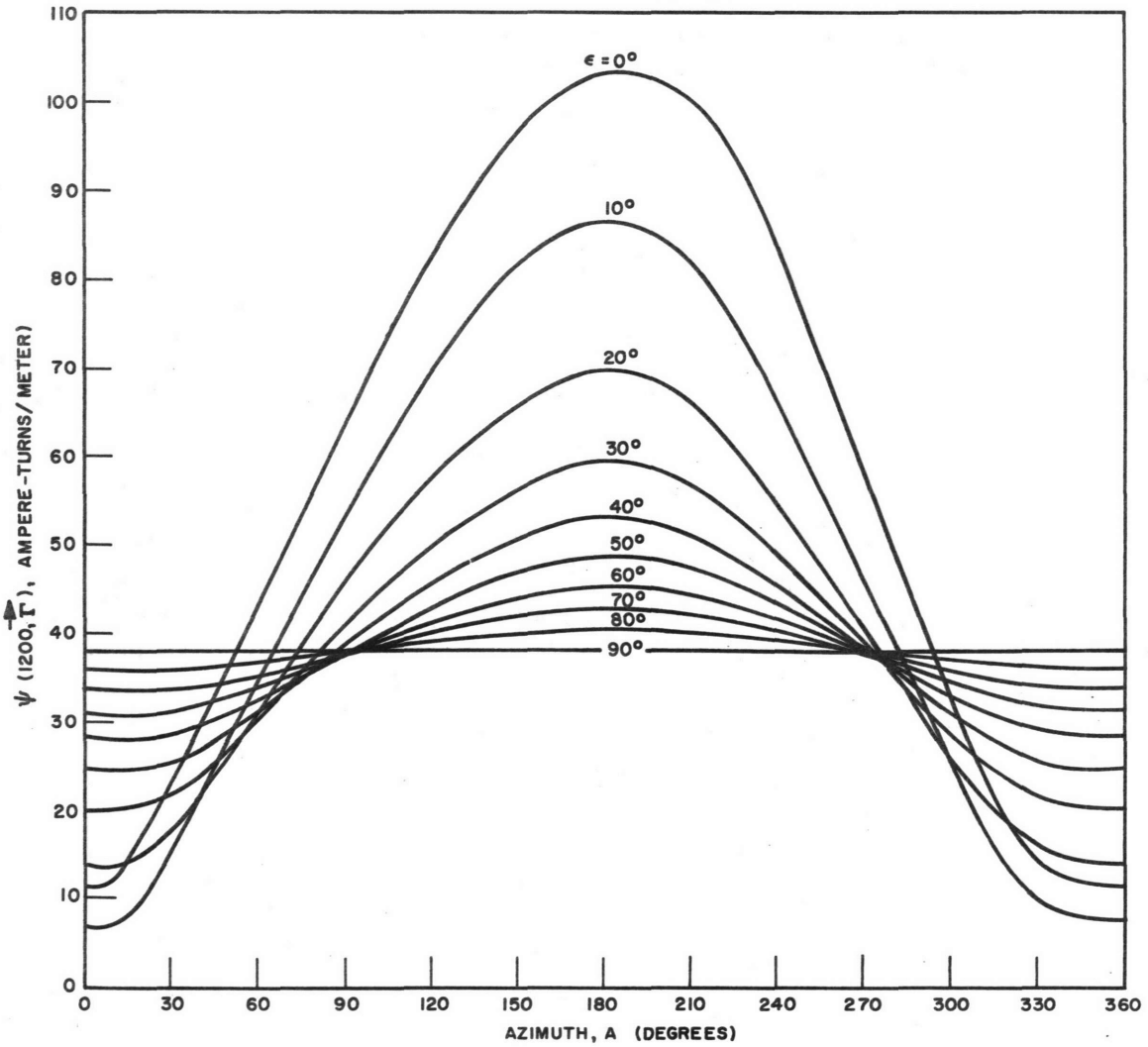

Fig. 33 - Magnetic field parameter for the Randle Cliff Radar site assuming $\bar{h}$ = 200 kilometers

14 and 70 ampere-turns/meter. For an equatorial site such as Kauai, Hawaii, $\bar{\psi}(\bar{h} = 200)$ varies between -25 and +60 ampere-turns/meter, and at Antigua, British West Indies, $\bar{\psi}(\bar{h} = 200)$ varies between -15 and +65 ampere-turns/meter. In the Southern Hemisphere the situation is reversed, the largest values of $\bar{\psi}(\bar{h} = 200)$ being negative.

Recall that $\tilde{\Omega}(f)$ at any one location is either clockwise (+) or counterclockwise (-); however, this does not imply that counterclockwise rotation may not occur for a location in which $\tilde{\Omega}(f)$ is positive or that clockwise rotation may not occur for a location in which $\tilde{\Omega}(f)$ is negative. The algebraic sign associated with $\tilde{\Omega}(f)$ denotes only the sense of the rotation of the plane of polarization for an earth-directed radar beam. It is true that the maximum change in the Faraday rotation angle is less than $|4\tilde{\Omega}|$ (since $|\Omega_{max}| \leq |2\tilde{\Omega}|$, and the change in rotation $\leq |2\Omega_{max}|$) and the maximum plausible number of Faraday fades exhibited by a train of radar pulses from a fixed-earth reference point is given by $4|\tilde{\Omega}|/\pi = 1.28\,|\tilde{\Omega}|$. Consequently, the maximum number of fades may be extracted from the charts of $\tilde{\Omega}$. In terms of losing the radar signal from a target at a specific location,

it is clear that there will be serious problems at 100 Mc/s; in fact, as many as 50 fades may occur at that frequency, whereas at 1000 Mc/s no more than one-half of a fade may occur.

PHASE SCINTILLATION

One of the more interesting features of the ionosphere is its structural irregularities. A variety of observational techniques show that irregularities exist in the ionosphere over all latitudes and occur throughout a wide altitude range. It is important to realize that the irregularities in the ionospheric electron content give rise to all types of scintillations such as amplitude, phase, polarization, angle of arrival, and range. Provided a knowledge of the phase effects is known, it is possible to estimate the other scintillation effects.

Regarding the irregularities which cause amplitude scintillation, increasing evidence indicates that patches of irregularities having a horizontal extent of as much as 400 kilometers occur, especially in the midlatitudes; and within these patches, smaller irregularities or inhomogeneities abound. The small-scale inhomogeneities are probably aligned with the earth's magnetic field and have an axial ratio of the order of 5:1 with their smallest dimension about a kilometer. Turbulence theory suggests that the inhomogeneities may only exist in the 200 to 300 kilometer altitude region (9), and the theory has been substantially verified by several investigators (10-12). One group has noted a uniform distribution with altitude (13), and workers at AFCRL have suggested that the scintillation region extends from 200 to 500 kilometers in altitude (14). Most workers agree that amplitude scintillation is predominantly a nocturnal phenomenon associated with spread F—the ionosonde terminology for a class of little understood F-region irregularities. Furthermore, it is rather well established that scintillation activity increases with both solar flux and magnetic activity. Whitney (15) suggests that at 130 Mc/s the scintillation index is roughly three times greater at sunspot maximum than at sunspot minimum and roughly three times greater at midnight than at noon. During summer a number of investigators noted that daytime scintillation is correlated with sporadic E (16, 17). Noisy scintillation associated with sporadic E may be caused by small inhomogeneities, but it is suggested that quasi-periodic scintillation is caused by a strong edge effect (18). It is noteworthy, however, that noisy scintillation is far more prevalent than the periodic variety.

The most useful information about the percentage change in content which constitutes an inhomogeneity has been derived from the Faraday rotation and doppler techniques. Other techniques incorporating the impedance probe, incoherent backscatter radar, and the topside sounder are also useful. Of these three, only the impedance probe has a reasonably good resolution.

It has been shown by Lawrence et al. (1) that the phase change introduced by the ionosphere is given by

$$\delta = -\frac{e^2}{4\epsilon_0 m\pi cf}\int_0^{h_s} N\,d\ell, \tag{7}$$

where e is the electronic charge, ϵ_0 is the free space permittivity, m is the electronic mass, c is the speed of light, f is the radio frequency, and ℓ is measured along the path of ray propagation. For the radar case, taking the average nadir angle effect into account, we find that, in mks units,

$$\delta(radians) = -1.7\times 10^{-14}\, n_f^{-1}\,\overline{\sec\chi}\int^{h_s} N\,dh, \tag{8}$$

where n_f represents the ratio (f/100 Mc/s). Since the amount of Faraday rotation for the radar case is given by

$$\Omega(radians) = 5.95 \times 10^{-2} f^{-2} \bar{\psi} \int_0^{h_s} N\, dh, \tag{9}$$

it follows that

$$|\delta/\Omega| = 2{,}857\, n_f \left[\overline{H \cos \theta}\right]^{-1}. \tag{10}$$

Assuming $H = 0.5$ gauss, it follows that $\left[\overline{H \cos \theta}\right]^{-1} = 0.025$ meter/ampere-turn when the ray path is directed along field lines. At 140 Mc/s, $n_f = 1.4$ and $|\delta| = 100\,|\Omega|$.

In some instances investigators quote percentage variations in the total content. For these cases it will be assumed that the same percentages apply for a satellite orbiting at an altitude of 300 kilometers. In addition it will be assumed that the subsatellite content is 10^{17} electrons/m^2. These assumptions might lead to overestimation of the degrading effects, but this is the proper course to take for the purposes of radar design. (The author admits to being biased on this point.) For a 1% variation in content, our assumptions imply that $\Delta\delta = -17$ radians at 100 Mc/s. In order to obtain a meaningful picture of the constraints placed upon the satellite radar by ionospheric irregularities, the author has taken the liberty to transform measured parameters into either scale length in kilometers (if it is not already) or phase change in radians. Furthermore, all data will be referenced to a radar frequency of 100 Mc/s. Of course, the author takes full responsibility for any incorrect interpretations. Figure 34 depicts the phase change for the radar case at 100 Mc/s as translated from the available data. The ordinate is in radians and the abscissa is in meters.

For the purpose of radar design the following law is suggested to describe the data represented in Fig. 34. Without regard to sign,

$$\frac{\Delta L}{\Delta\delta \cdot n_f} \approx 10^3, \tag{11}$$

where ΔL is the horizontal scale in meters and $\Delta\delta$ is the phase change in radians. This relation implies that typical irregularities with scales of the order of 1 kilometer describe a phase change of 1 radian and implies that irregularities with scales of 100 kilometers produce a phase change of about 100 radians. At 1000 Mc/s, $n_f = 10$, which implies that 1-kilometer-scale irregularities cause a phase excursion of at most 1/10 radian or about 6°.

It is anticipated that these irregularities would be more prevalent by night than by day and would appear more often as solar and/or magnetic activity increase. There is also much evidence that Eq. (11) would be inappropriate in the auroral region. Perhaps $\Delta L/\Delta\delta \cdot n_f = 10^2$ would be more reasonable for scales of the order of a few kilometers.

The mean-square phase fluctuations $\overline{(\Delta\delta)^2}$ have been discussed by Lawrence et al. (1) and Millman (2) assuming a uniform distribution of inhomogeneities with vertical scale Δh. From this analysis it may be shown that

$$\overline{(\Delta\delta)^2} = 2(\pi/\lambda)^2 D \cdot \Delta h (f_p/f)^4 \overline{(\Delta N/N)^2}, \tag{12}$$

where D is the ionospheric vertical thickness, f_p is the plasma frequency, f is the radar frequency, and $\Delta N/N$ is the fractional density variation. Figure 35 consists of curves of $\overline{(\Delta\delta)^2}$ for a radar frequency of 100 Mc/s as a function of $D \cdot \Delta h$ with $\left[(f_p/f)^4 \cdot \overline{(\Delta N/N)^2}\right]$ as parameter. Assuming a mean-square density fluctuation of $\overline{(\Delta N/N)^2} = 10^{-4}$, an irregularity

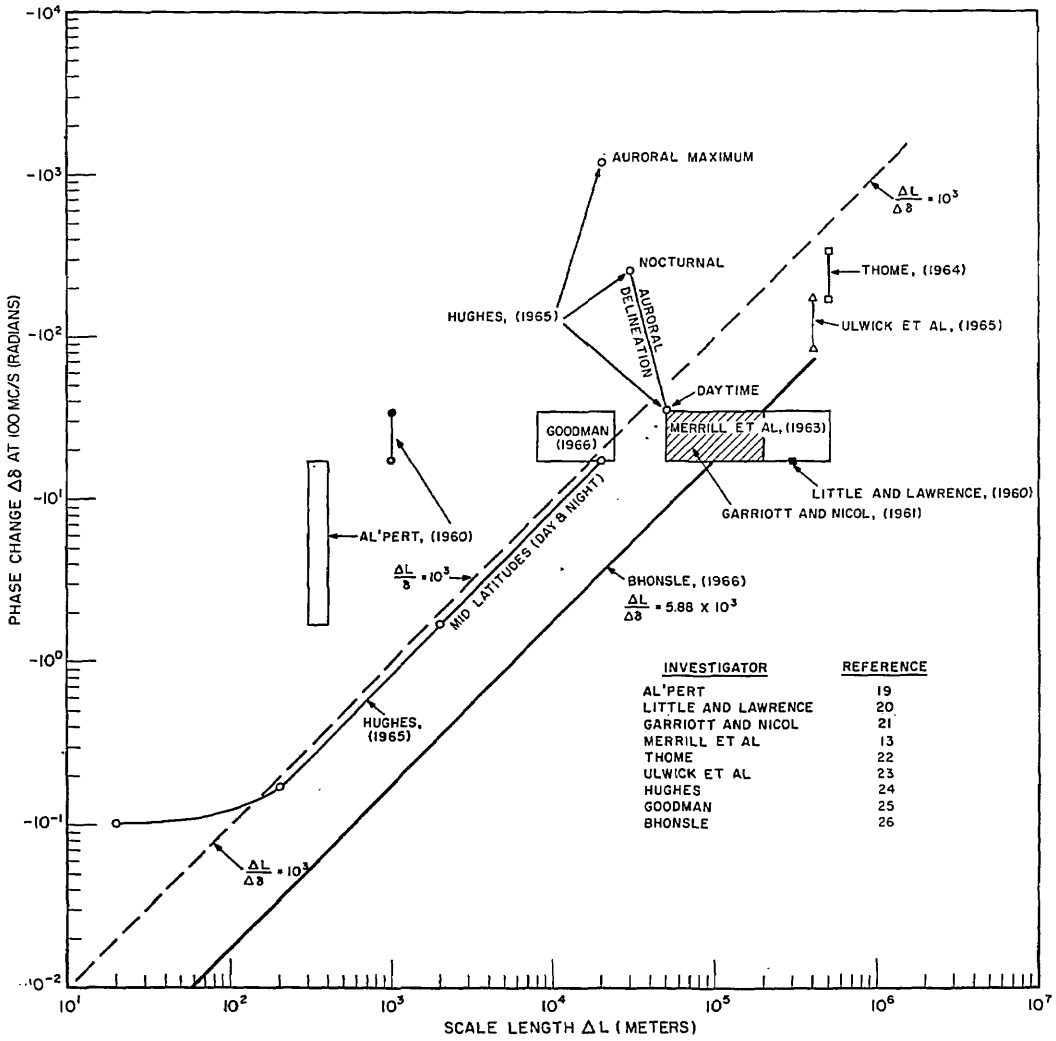

Fig. 34 - Phase change $\Delta\delta$ at 100 Mc/s versus horizontal scale length. In all cases investigators used frequencies other than 100 Mc/s, and in most cases an electron content excursion (in percentage turns) was stated. Hughes' data at 162 Mc/s was expressed in terms of phase change versus horizontal scale and was transformed to 100 Mc/s by applying the frequency relation $\delta \propto f^{-1}$. Y. Al'pert's data was derived from dispersive doppler techniques at hf. He notes that electron content inhomogeneities exist but characterized them by an electron density excursion $(\Delta N/N)$. By assuming that $(\Delta N/N) \propto (\Delta C/C)$ and using the frequency relation, Al'pert's deductions were transformed to a 100 Mc/s total content basis and consequently may be overestimates. It is noteworthy that the phrase "a few percent" was interpreted as a phase variation of between -17 and -34 radians at 100 Mc/s. A phase change of -17 radians at 100 Mc/s corresponds to $\Delta C = 10^{15}$ electrons/m^2, or a 1% change, assuming that $C = 10^{17}\ m^{-2}$.

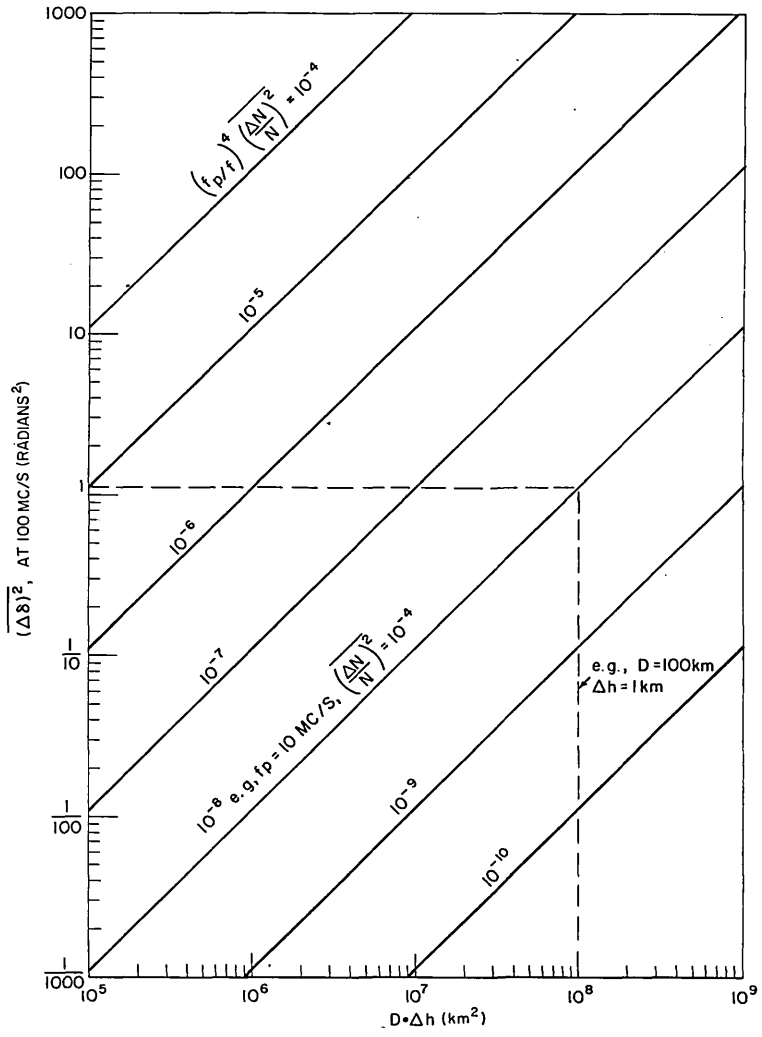

Fig. 35 - Mean-square phase change at 100 Mc/s versus $D \cdot \Delta h$ with $\left[(f_p/f)^4 \cdot \overline{(\Delta N/N)^2}\right]$ as parameter. f_p is the plasma frequency, f is the radar frequency, $\Delta N/N$ is the electron density fractional excursion, D is the ionospheric slab over which irregularities exist, and Δh is the horizontal scale of the irregularities.

vertical scale of Δh = 1 kilometer, a slab thickness (over which the irregularities exist) of D = 50 kilometers, and a plasma frequency f_p = 10 Mc/s, we see that Eq. (12) yields a value for the rms phase fluctuation of approximately 1 radian at 100 Mc/s or 1/10 radian at 1000 Mc/s. This is in agreement with the law $\Delta L/\Delta\delta \cdot n_f = 10^3$. Generalizations resulting from a blind use of Eq. (12) should be avoided, since it was derived on the basis of spherical irregularities distributed in a uniform fashion. Keeping this in mind, however, one may derive some upper limits for the rms phase fluctuations at any radar frequency.

It has been shown by the author (26) that, for a circularly orbiting satellite, the horizontal scale of an inhomogeneity is related to the disturbance duration Δt by the relation

$$\Delta L = 19.95 \times 10^6 \, (r_e + h_s)^{-1/2} \, (h_i/h_s) \, \Delta t \; (mks\ units), \tag{13}$$

where r_e is the radius of the earth, h_i is the height of the inhomogeneity, and h_s is the height of the satellite. For a satellite radar operating at an altitude of 300 kilometers, it may be shown that $\Delta L = 2.57 \times 10^{-2}\ h_i\ \Delta t$; and if the inhomogeneity height is approximately 200 kilometers, a time duration of 1 second corresponds to roughly 5 kilometers. Consequently, if typical horizontal scales are 1 kilometer and the inhomogeneities have a mean altitude of 200 kilometers, then on the basis of Eq. (11) it is easily shown that a phase variation of greater than 5 radians may occur in 1 second at 100 Mc/s. At 1000 Mc/s the time rate of change of phase might be greater than 1/2 radian/second. These are obviously upper limits, and one might wish to put more faith in the limited data which are available. It is interesting that Hughes (25) has detected typical phase fluctuations at 162 Mc/s of approximately 1 radian over 2 kilometers in the midlatitudes, which corresponds to a phase change rate of greater than 2 radians/second.

CONCLUSION

With regard to the Faraday rotation problem, it has been shown that $\tilde{\Omega}$, which is not less than 1/2 the maximum Faraday rotation angle, is relatively constant on a worldwide scale for a given radar frequency. The beam orientation is, however, crucial if one wishes to estimate the exact amount of rotation for a satellite situated at a particular point in space. The number of Faraday fades which are likely to occur over a particular field station is generally quite large for a high-inclination satellite. The number of fades will decrease with decreasing inclination of the satellite orbit.

It is shown that the maximum number of fades exhibited by a train of radar pulses is approximately 1.28 $|\tilde{\Omega}|$, where $\tilde{\Omega}$ is in radians. At 100 Mc/s it was found that the maximum number of fades is characteristically less than 50. Consequently, at 1000 Mc/s no more than one-half of a fade should occur, since $\Omega \propto f^{-2}$. Faraday rotational degradation of a linearly polarized radar signal has been found to be negligible at 1000 Mc/s except possibly during winter days when solar activity is high. This problem may be avoided completely by transmitting and receiving circular polarization. In all but possibly the polar region, it is suggested that the relationship between irregularity scale ΔL and phase excursion $\Delta\delta$ is given by

$$\frac{\Delta L}{\Delta\delta \cdot n_f} = 10^3,$$

where ΔL is in meters, $\Delta\delta$ is in radians, and n_f is the radar frequency in hundreds of megacycles per second. In the auroral and polar regions $\Delta L / \Delta\delta \cdot n_f = 10^2$ is probably more reasonable for the small scales.

One of the areas which has not been considered is that of amplitude scintillation. For years the scintillation of radio stars due to ionospheric irregularities—not unlike the twinkling of "optical" stars due to tropospheric winds—has been intensively investigated. Amplitude scintillation has been shown to be quite pronounced, especially at vhf during nocturnal hours, and is particularly violent in the auroral zone. However, for the satellite radar case under consideration in this report, if we denote the relative distances between the satellite and the inhomogeneities by Z' and between the inhomogeneities and the surface by Z, clearly Z and Z' play a major role in the incomplete development of amplitude scintillations. Since the depth of amplitude fading A is proportional to $[Z'/(Z' + Z)]^2$, it follows that for a satellite orbiting at an altitude of 300 kilometers above a patch of inhomogeneities located at an altitude of 200 kilometers, A is 19 dB. If the altitude of the inhomogeneities is 250 kilometers, then A is 31 dB. It is clear that one would expect little or no scintillation for the 300 kilometer radar case unless irregularities were located at E-region height. In this regard it is possible that sporadic E patches in temperate latitudes, the equatorial electrojet, and the auroral activity may produce nonnegligible amplitude effects. They are certainly fruitful areas for more research. Special attention

is called to the work of Aarons at AFCRL and in particular to Whitney's paper (15) which is a summary of Air Force work in the field of tropospheric and ionospheric scintillation as related to synchronous satellite radiowave transmissions.

It is emphasized that the results presented in this report are weighted toward the prediction of the maximum plausible values of Faraday rotation, Faraday fading, and phase distortion. This approach is the only meaningful one, since available data is not sufficiently extensive to render a satisfactory statistical approach to the estimation of these quantities. Although a "law" such as $\Delta L/\Delta\delta \cdot n_f \approx 10^3$ gives us some feeling for the relationship between irregularity scale and phase excursion, it is important to realize what it does not tell us. It does not, for example, tell us the probability of occurrence of any particular scale length nor does it tell us the diurnal, seasonal, or sunspot epochal variations of these probabilities. In order to obtain a meaningful picture of the ionospheric irregularity structure, these aspects must be investigated.

ACKNOWLEDGMENTS

R. E. Ellis suggested varying the radar beam orientation for the Faraday rotation analysis, and LCDR Hilder of the Bureau of Weapons suggested incorporating a discussion of possible phase effects. Mrs. S. J. Rutiser is acknowledged for programming the formulas necessary for the Faraday analysis, and J. W. Wright of ESSA is thanked for his suggestions concerning the prediction of electron content.

REFERENCES

1. Lawrence, R.S., Little, C.G., and Chivers, H.J.A., "A Survey of Ionospheric Effects Upon Earth-Space Radio Propagation," Proc. of the IEEE 52:4 (Jan. 1964)

2. Millman, G.H., "A Survey of Tropospheric, and Extraterrestrial Effects on Radio Propagation Between the Earth and Space Vehicles," G.E. Report R66EMH1, Jan. 1966

3. Yeh, K.C., and Gonzalez, V.H., "Note on the Geometry of the Earth Magnetic Field Useful to Faraday Effect Experiments," J. Geophys. Res. 65:3209 (Oct. 1960)

4. Goodman, J.M., "Prediction of Faraday Rotation Angles at VHF and UHF," NRL Report 6234, Apr. 28, 1965

5. Mitra, S.K., "The Upper Atmosphere," The Royal Asiatic Society of Bengal, Calcutta, India, pp. 141-327 (1947)

6. Shimazaki, T., "A Theoretical Study of the Dynamical Structure of the Ionosphere," J. Rad. Res. Lab. 6:107-241 (Mar. 1959)

7. Seddon, J.C., "A Model of the Quiet Ionosphere," J. Geophys. Res. 68:1339 (Mar. 1, 1963)

8. Wright, J.W., private communication, Sept. 15, 1966

9. Booker, H.G., in "Polar Atmosphere Symposium," Part II, London:Pergamon Press, p. 52, 1957

10. Rao, P.B., and Rao, B.R., "Height Variation of Drift and Anisotropy of the Ionospheric Irregularities," J. Atmospheric Terrest. Phys. 26:231 (1964)

11. Rao, B.R., and Romana, K.V.V., Proceedings of the IGY Symposium, C.S.I.R., New Delhi, India, 1961

12. Lawrence, J.D., Jr., and Martin, J.D., "Diurnal, Seasonal, Latitudinal, and Height Variations of Satellite Scintillation," J. Geophys. Res. 69:1293 (Apr. 1, 1964)

13. Merrill, R.G., Lawrence, R.S., and Roper, N.J., "Synoptic Variations and Vertical Profiles of Large-Scale Ionospheric Irregularities," J. Geophys. Res. 68:5453 (Oct. 1, 1963)

14. Allen, R.S., Aarons, J., and Whitney, H., "Measurements of Radio Star and Satellite Scintillations at a Subauroral Latitude," IEEE Transactions on Military Electronics, MIL-8:146 (July-Oct. 1964)

15. Whitney, H.E., "The Relationship of 50 Mc - 250 Mc Scintillations to Satellite to Ground Communications," Briefing to OAR, Feb. 1, 1966, Washington, D.C.

16. Goodman, J.M., "Diurnal Dependence of Electron Content Variations," J. Geophys. Res. 71:985 (Feb. 1, 1966)

17. Dagg, M., "Radio-Star Ridges," J. Atmospheric Terrest. Phys. 11:118 (1957)

18. Goodman, J.M., "Some Evidence of E_s Layer Effects Upon 137 MHz Radio Waves," (To be published in J. Atmospheric Terrest. Phys.)

19. Alpert, Y.L., "Investigation of the Ionosphere and the Interplanetary Gas with the Aid of Artificial Earth Satellites and Space Rockets," translated from the Russian, in Artificial Earth Satellites Vols. 7 and 8, pp. 125-165 (June 1962)

20. Little, C.G., Lawrence, R.S., "The Use of Polarization Fading of Satellite Signals to Study the Electron Content and Irregularities in the Ionosphere," J. Res. Nat'l. Bur. Std. 64D:335 (1960)

21. Garriott, O.K., Nicol, A.W., "Ionospheric Information Deduced From the Doppler Shifts of Harmonic Frequencies from Earth Satellites," J. Atmospheric Terrest. Phys. 22:50 (1961)

22. Thome, G.D., "Incoherent Scatter Observations of Traveling Ionospheric Disturbances," J. Geophys. Res. 69:4047 (Oct. 1, 1964)

23. Ulwick, J.C., Pfister, W., McInerney, R.E., "Direct Satellite Probe Measurements of Ionospheric Irregularities," in "Space Research V," New York:North-Holland, pp. 171-188, 1965

24. Hughes, L.R., "Parameters of a Cloud-Like Distribution of Electrons in the Ionosphere," paper presented at the Second Symposium on Radio Astronomical and Satellite Studies of the Atmosphere, Boston, Mass., Oct. 1965

25. Goodman, J.M., "On the Determination of Fine Scale Ionospheric Inhomogeneities by Means of a Faraday Rotation Analysis of Echo II Radar Returns," NRL Memorandum Report 1723, Sept. 19, 1966

26. Bhonsle, R.V., "Diurnal Variation of Large-Scale Ionospheric Irregularities," J. Geophys. Res. 71:4571 (Oct. 1, 1966)

Security Classification

DOCUMENT CONTROL DATA - R & D

Security classification of title, body of abstract and indexing annotation must be entered when the overall report is classified)

1. ORIGINATING ACTIVITY *(Corporate author)* Naval Research Laboratory Washington, D.C. 20390	2a. REPORT SECURITY CLASSIFICATION Unclassified 2b. GROUP

3. REPORT TITLE

A NOTE ON THE POLARIZATION AND PHASE CHARACTERISTICS OF RADIO WAVES PROPAGATING THROUGH THE LOWER IONOSPHERE

4. DESCRIPTIVE NOTES *(Type of report and inclusive dates)*

A final report on the problem; work on the problem is completed.

5. AUTHOR(S) *(First name, middle initial, last name)*

John M. Goodman

6. REPORT DATE June 5, 1967	7a. TOTAL NO. OF PAGES 38	7b. NO. OF REFS 26
8a. CONTRACT OR GRANT NO. NRL Problem R07-16 b. PROJECT NO. RT 7042-045/6521/F019-02-18 c. d.	9a. ORIGINATOR'S REPORT NUMBER(S) NRL Report 6532 9b. OTHER REPORT NO(S) *(Any other numbers that may be assigned this report)*	

10. DISTRIBUTION STATEMENT

Distribution of this document is unlimited.

11. SUPPLEMENTARY NOTES	12. SPONSORING MILITARY ACTIVITY Department of the Navy (Office of Naval Research), Washington, D.C. 20360

13. ABSTRACT

Some ionospheric radio propagation problems associated with the satellite radar situation have been examined for radar frequencies between 100 and 1000 Mc/s. It has been shown that the maximum number of fades exhibited by a train of radar pulses is governed by the quantity $\overline{H \csc I}$, where H is the magnetic field intensity and I is the magnetic field inclination, except near the magnetic equator. At 100 Mc/s the maximum number of fades is characteristically less than 50, and since the Faraday rotation is inversely proportional to the square of the radar frequency, only one-half of a fade should be observed at 1000 Mc/s.

Faraday rotational signal degradation of a linearly polarized radar signal has been shown to be negligible at 1000 Mc/s except possibly during winter days at sunspot maximum. In all but possibly the polar region, it is suggested that the relationship between irregularity scale ΔL and phase excursion $\Delta\delta$ is given by

$$\frac{\Delta L}{\Delta\delta \cdot n_f} \approx 10^3,$$

where ΔL is in meters, $\Delta\delta$ is in radians, and n_f is the radar frequency in hundreds of megacycles per second.

DD FORM 1 NOV 65 1473 (PAGE 1)

S/N 0101-807-6801

Security Classification

14 KEY WORDS	LINK A ROLE	LINK A WT	LINK B ROLE	LINK B WT	LINK C ROLE	LINK C WT
Faraday effect (magneto-ionic)						
Polarization						
Satellite						
Radar						
Phase						
Inhomogeneities (irregularities)						
Electron content						